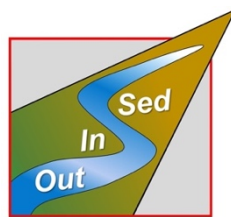


SedInOut: Development of a risk management methodology by assessing the availability of sediment for transport in mass in mountain environments

SedInOut



Development of a risk management methodology by assessing the availability of sediment for transport in mass in mountain environments

WP7

Development of Manuals and Guidelines

October 2022



German: <https://www.provinz.bz.it/bauen-wohnen/oeffentliche-bauten/geologie/projekt-sedinout.asp>

Italian: <https://www.provincia.bz.it/costruire-abitare/edilizia-pubblica/geologia/progetto-sedinout.asp>

Legal notice:

This guide was produced as part of the Interreg V-A Italy-Austria SedInOut project. The SedInOut project was funded by the Interreg V-A Italy- Austria 2014 - 2020 program.

Texts, images, and layout:

Project partners

- [Amt für Geologie und Baustoffprüfung](#) - Autonome Provinz Bozen
- [Regione del Veneto](#) - Direzione Difesa del Suolo U.O. Geologia
- [Regione Autonoma Friuli-Venezia Giulia](#) - DIREZIONE CENTRALE, DIFESA DELL'AMBIENTE, ENERGIA E SVILUPPO SOSTENIBILE. SERVIZIO GEOLOGICO
- [Amt der Salzburger Landesregierung](#) - Abteilung 6 Infrastruktur und Verkehr
- [Amt der Kärntner Landesregierung](#) - Abteilung 8 - Umwelt, Energie und Naturschutz



AUTONOME
PROVINZ
BOZEN
SÜDTIROL



PROVINCIA
AUTONOMA
DI BOLZANO
ALTO ADIGE



REGIONE DEL VENETO



REGIONE AUTONOMA
FRIULI VENEZIA GIULIA



LAND
SALZBURG



LAND KÄRNTEN

Scientific affiliates

- [Università di Bologna](#) Dipartimento di Scienze Biologiche, Geologiche e Ambientali (BIGEA)
- [Università di Milano](#): Dipartimento di Scienze dell'Ambiente e della Terra (DISAT)
- [l'Istituto di Ricerca per la Protezione Idrogeologica del Consiglio Nazionale delle Ricerche \(CNR Irpi\)](#):
Sede di Padova - Istituto di Ricerca per la Protezione Idrogeologica
- [Georesearch GmbH](#)
- [Technische Universität Graz](#)



ALMA MATER STUDIORUM
UNIVERSITÀ DI BOLOGNA



Istituto di Ricerca per la Protezione Idrogeologica



UNIVERSITÀ DEGLI STUDI
DI MILANO
BICOCCA



GEORESEARCH



Table of contents

Introduction.....	7
Focus	9
Summary	9
Measurement and recording methodology.....	10
Decision-making process.....	16
Final products	17
Checklist.....	17
Determination of grain size distribution by means of photogrammetry	19
Focus	19
Summary	19
Measurement and recording techniques.....	20
Final Product	22
Decision making progress	22
Example	23
Geomorphological analysis	26
Focus	26
Summary	26
Measurement and recording methodologies.....	27
Main characteristics	28
Materials and texture	30
Geometry.....	32
Final products	36
Decision-making progress: Guideline for identifying debris flows.....	37
Evaluation of remobilization of sediment (debris fans).....	39
Focus	39
Measurement and recording techniques.....	40
Model generation	40
Grain size distribution and shape of particles	40
Modelling of the area under investigation	41
Selection of micro parameters and scaling.....	42
Hazard modelling	42

Rock fall.....	42
Rainfall	43
Seismicity.....	43
Final products	43
Decision-making progress.....	43
Example	44
Field-based data retrieval	50
Focus	50
Summary	50
Measurement and recording methodologies.....	51
Description of the deposits	51
Survey of mountain rivers.....	55
Final products	60
Construction of the complete grain-size curve of the deposit	60
Checklist.....	64
Field form for the characterization of deposits.....	64
Field form for the characterization of mountain-river course.....	65
Sediment Analysis.....	66
Focus	66
Summary	66
Measurement and recording methodology.....	67
Field-based analysis	67
Surface GSD.....	68
Subsurface GSD	70
Laboratory-based analysis	71
Los Angeles Abrasion test	71
Granulometry.....	73
Software-based analysis	74
Final products	78
.....	79
Decision-making process.....	86
Checklist.....	86
Sediment use	89
Focus	89











Summary	89
Railway ballast	90
Particle characteristics	90
Mechanical/physical properties.....	91
<i>Fragmentation resistance - Los Angeles (LA) test</i>	91
Lithological classification	92
Gabions.....	92
Geometric characteristics.....	92
Fine aggregate for concrete (ASTM)	92
Particle characteristics	92
Dangerous substances	92
Soundness.....	93
Coarse aggregates for concrete (ASTM)	93
Geometric characteristics.....	93
Dangerous substances	94
Aggregates for asphalts (Washington Department of Transportation 2004)	95
Particle characteristics	95
Physical characteristics.....	95
Portland cement (UNI-EN).....	95
Soil correction (ASTM).....	97
Particle size characteristics	97
Bibliography	98

Introduction

This manual has been established during the Interreg V Italy-Austria project SedInOut (funding period 2014-2020).

Project specific outcomes are reached via the transregional cooperation of the following partners and institutions (Table 1).

Table 1. Project partners and scientific affiliates.

Abbreviation	Project partner	Logo	Scientific affiliates	Logo
LP	Amt für Geologie und Baustoffprüfung (Autonome Provinz Bozen)		Università Bologna (BiGea)	
PP1	Regione del Veneto		CNR IRPI Padova	
PP2	Regione Friuli-Venezia Giulia		Università Milano (Bicocca)	
PP3	Land Salzburg		Georesearch GmbH	
PP4	Land Kärnten		Universität Graz	

The joint analysis, assessment, and information system, which is being developed within the institutional cooperation between all partners, results in a new concept for upgrading the cooperation of administrations, which allows a transboundary and standardized assessment of debris flows occurrence and the appropriate protection measures in the whole EUREGIO area and beyond.

The guide contains the outputs of work package 7 (WP7) and aims to present common, shared, and standardized methodologies, while integrating concepts of already available measures. Thereby, the project approach is designed to maximize the quality of the results and to minimize the costs for the institutions and authorities involved in the tasks of monitoring the territory. In this regard, WP7 comprises the following activities (best practice approach, user-friendly manual):

- 1- Development of a conceptual model of sediment mobilization and transport at basin scale. The model is based on the results obtained in WP4 and WP5.
- 2- Development of guidelines and a manual for defined, harmonized, and standardized workflows depending on the available source data and the meteorological characteristics of the area of interest (WP3).
- 3- Development of guidelines and manuals for the characterisation and sustainable management of the sediment (WP5).
- 4- Proposals for the amendment of sector regulations of regional competence for the recovery of materials transported and deposited in riverbeds as raw materials.

The guide summarizes the main work package outputs. The main aspects of each topic are presented in singular chapters. These sections were elaborated under the cure of the responsible project partners (Table 2).

Table 2. Work packages, respective chapters, and responsible partners.

<i>Work package</i>	<i>Chapter</i>	<i>Responsible partner</i>
WP3	Remote Sensing	PP3
	Determination of grain size distributions by means of photogrammetry	PP4
WP4	Geomorphological analysis	PP1
	Evaluation of the remobilisation of sediment (debris fans)	PP4
	Field-based data retrieval	PP2
WP5	Sediment characterisation	LP
WP6	Sediment analysis	LP
WP7	Sediment use	PP2

Remote Sensing

Focus

This chapter is about a remote sensing-based detection of alpine mass movements in loose material. Here, the focus is on the creeping and sliding slopes. According to the definition by Krauter (1990), the velocity range is between mm per year and m per year (**Error! Reference source not found.**).

Prozessart	Geschwindigkeitsbereich nach Krauter (1990) & Häfeli (1967)	Bezeichnungen (Beispiele)
Kriechen	mm pro Jahr bis mm pro Tag	Bodenkriechen, Schuttkriechen, Blockkriechen, Schuttstromkriechen
Gleiten/Rutschen	mm pro Jahr bis m pro Stunde	Felsgleitung, Bodenrutschung, Schuttrutschung
Fließen	m/s	Schlammstrom, Erdstrom, Schuttstrom, Mure
Fallen/Stürzen	größer als 20 m pro Sekunde	Bergsturz, Felssturz, Blocksturz, Steinfall
Komplex	Komplex und variabel	
- Kriechen/Gleiten/Rutschen	mm pro Jahr bis mm pro Tag	Talzus Schub , Bergerrei ßung, Sackung
- Kriechen/Gleiten/Rutschen	mm pro Jahr	Blockbewegung

Figure 1. Definition of gravitational processes with velocity ranges (GBA 2002; Krauter, 1990).

To detect these movements, there is a wide range of remote sensing methods, which is described more detailed within this chapter. However, in the SedInOut project the main method used was the satellite based InSAR (Interferometric Synthetic Aperture Radar) analysis. The available data includes mainly the spectral and multispectral satellite data, the X-, C- and L-band radar satellite data and the ALS (Airborne Laser Scanning) data of the federal states. In addition, it is possible to enhance these data types with helicopter-based or drone-based surveys with high-resolution datasets. However, in comparison to the mentioned data types, these data records are not permanently available over a wide area.

Summary

Remote sensing is a powerful tool for the detection and quantification of mass movements in alpine regions. Within the Interreg SedInOut Project a best practice approach for this application has been developed. This chapter serves as an overview and description of the different methods and products which are used in the field of remote sensing. The focus is mainly on the InSAR analysis since this was the base dataset in this project. New knowledge and data sets are presented and applied in a practical

example. A checklist and comprehensive tables help to make decisions when applying these methods. The results from the InSAR analysis are available online at <https://www.salzburg.gv.at/sagismobile/sagisonline/map/Bauen%20und%20Wohnen/InSar>.

Measurement and recording methodology

InSAR Methodology

Satellite-based InSAR (Interferometric Synthetic Aperture Radar) is currently the only method to detect ground motion and deformation precisely and directly (mm accuracy), in a scalable way (from single building to vast areas) and over long periods of time (from less than one up to 25 years, historical archives). Systematic ground deformation measuring from space is possible since the launch of the satellite ERS-1 by the European Space Agency (ESA) in 1992 (Ferretti 2007). Nowadays we have several radar satellite systems which measure in a continuous manner the whole globe. There are satellite systems like COSMO-SkyMed, TerraSAR-X, Radarsat-1, ENVISAT, ALOS-1, Sentinel-1 and more. They all are working with a Synthetic Aperture Radar (SAR) system, but the radar image results are different in terms of resolution, coverage, and revisiting time. (Dörfler 2020; 2022)

Table 3 lists the different types of radar satellites. It shows an increase within the GHz value from L-band to X-band, connected with a decrease in its wavelength. The wavelength is an important factor in deciding which satellite is suitable for a particular problem. It determines which objects are detected as reflectors and which are not. Objects smaller than half of the wavelength will not be recognized. The wavelength is also decisive for the penetration capability of the radar wave. For example, an L-band signal penetrates vegetation much better than an X-band signal (Ferretti 2014).

Table 3. Specifications of the different SAR sensors (TRE ALTAMIRA 2018).

Band	Frequencies	Wavelengths	Sensors
L	1 – 2 GHz	30 – 15 cm	SEASAT, JERS-1, ALOS-PALSAR
S	2 – 4 GHz	15 – 7.5 cm	HJ-1
C	4 – 8 GHz	7.5 – 3.75 cm	ERS-1, ERS-2, RADARSAT-1, RADARSAT-2, ENVISAT, Sentinel-1
X	8 – 12 GHz	3.75 – 2.5 cm	COSMO-SkyMed, TerraSAR-X, Tandem-X

Table 4 shows past and present SAR satellite systems. An increasing number of satellite systems have been launched over the last two decades. Liao et al. (2020) describes that this fact is also a reason for the strongly increasing number of InSAR publications.

Table 4. Overview of the past and present SAR satellite systems (Liao et al. 2020).

SENSOR	BAND	PERIOD	ORGANIZATION/ COUNTRY
<i>Seasat</i>	L	1978	NASA
<i>ERS-1/2</i>	C	1991-2011	ESA
<i>JERS-1</i>	L	1992-1998	JAXA
<i>Radarsat-1</i>	C	1995-2013	CSA
<i>Envisat/ASAR</i>	C	2002-2012	ESA
<i>ALOS PALSAR</i>	L	2006-2011	JAXA
<i>Cosmo-SkyMed</i>	X	2007-present	ASI
<i>TerraSAR-X</i>	X	2007-present	DLR
<i>HJ-1C</i>	S	2012-2013	China
<i>Kompsat-5</i>	X	2013-present	Korea
<i>Radarsat-2</i>	C	2014-present	CSA
<i>ALOS-2</i>	L	2014-present	JAXA
<i>Sentinel-1</i>	C	2014-present	ESA
<i>GF-3</i>	C	2016-present	China
<i>PAZ</i>	X	2018-present	Spain
<i>SAOCOM</i>	L	2018-present	Argentina
<i>ICEEYE-X</i>	X	2018-present	Finland/Poland
<i>Radarsat Constellation</i>	C	2019-present	CSA

Since the first radar satellite ERS-1 the InSAR-technology has improved steadily in terms of resolution, return period, coverage and, above all, the evaluating algorithms. Nowadays SB-InSAR is a proven technology. Since 2014, the launch of ESA's satellite Sentinel-1, satellite radar images are freely available, and the return period of the satellites improves to 6-day intervals. Also the publications and citations of InSAR topics are raising very fast since this time (Novellino et al. 2017; Liao et al. 2020). Satellite based InSAR is now used in a lot of different applications like groundwater subsidence monitoring (Osmanoğlu et al. 2011), landslide detection (Intrieri et al. 2018), reservoir monitoring (Ferretti 2014), civil engineering (Koudogbo 2018; Bischoff et al. 2020), and more. Especially in the field of civil engineering nowadays InSAR is used as a state-of-the-art method. (Liao et al. 2020)

Due to the increasing use in the last years, some very clear advantages and disadvantages have become apparent. The advantages of this method are that historical data is available and that the data usually covers very large areas. The SAR satellites are active systems which can record data even during cloud cover and at night. In addition, there is no need to take in situ measurements, which can save a lot of time. But there are also disadvantages, it is currently almost impossible to measure strongly vegetated areas with InSAR. Also, fast, or abrupt movements are not measurable, because they either lose their shape or the radar signal suffers phase jumps. (Dörfler 2021; Liao et al. 2020).

Project results of the InSAR analysis

Within the SedInOut project satellite data of the Sentinel-1 mission was used to determine hotspots of slow mass movements in the project AOI. Therefore 230 satellite images from the ascending mode and 264 images from the descending mode was analysed for the time slot of 2015 - 2020. The processing algorithm used for the unwrapping of the interferograms was the SqueeSAR® (Ferretti 2011) algorithm of TRE ALTAMIRA. The result is a dataset of about 2.8 million measurement pixels, which all include a timeseries of at least 230 timestamps. However, the following figure gives an overview of the huge number of measurement results. Even within this overview scale, certain large mass movements are already noticeable, such as the large slope movement near Krimml (a.), the mass movement at the Wasserradkopf (b.) and the landslides in the cirques above the Muhr valley (c.). This method therefore has the potential to give a quick overview of motion hotspots over large areas.

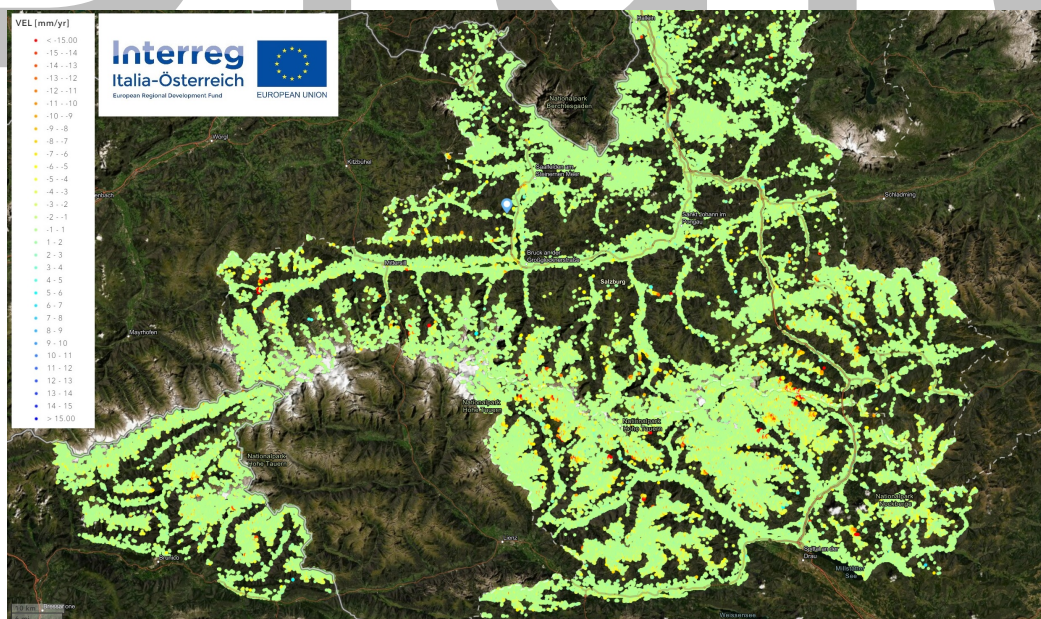


Figure 2. Results of the Sentinel-1 based InSAR analysis within the AOI (area of interest) of the SedInOut project.

Coming from this overview, the following figure shows a detailed view of the results at the Wasserradkopf. Here two different algorithms (SqueeSAR® and FASTVEL) were compared. While SqueeSAR® has a very strong potential in detecting movements with millimetre accuracy, the limits of the algorithm can be reached for very fast movements, like those at the Wasserradkopf. To complement these results, other algorithms, such as FASTVEL (FASTVEL 2022) can be used. These do not reach such precise measurement values by far, but they are able to detect faster movements.

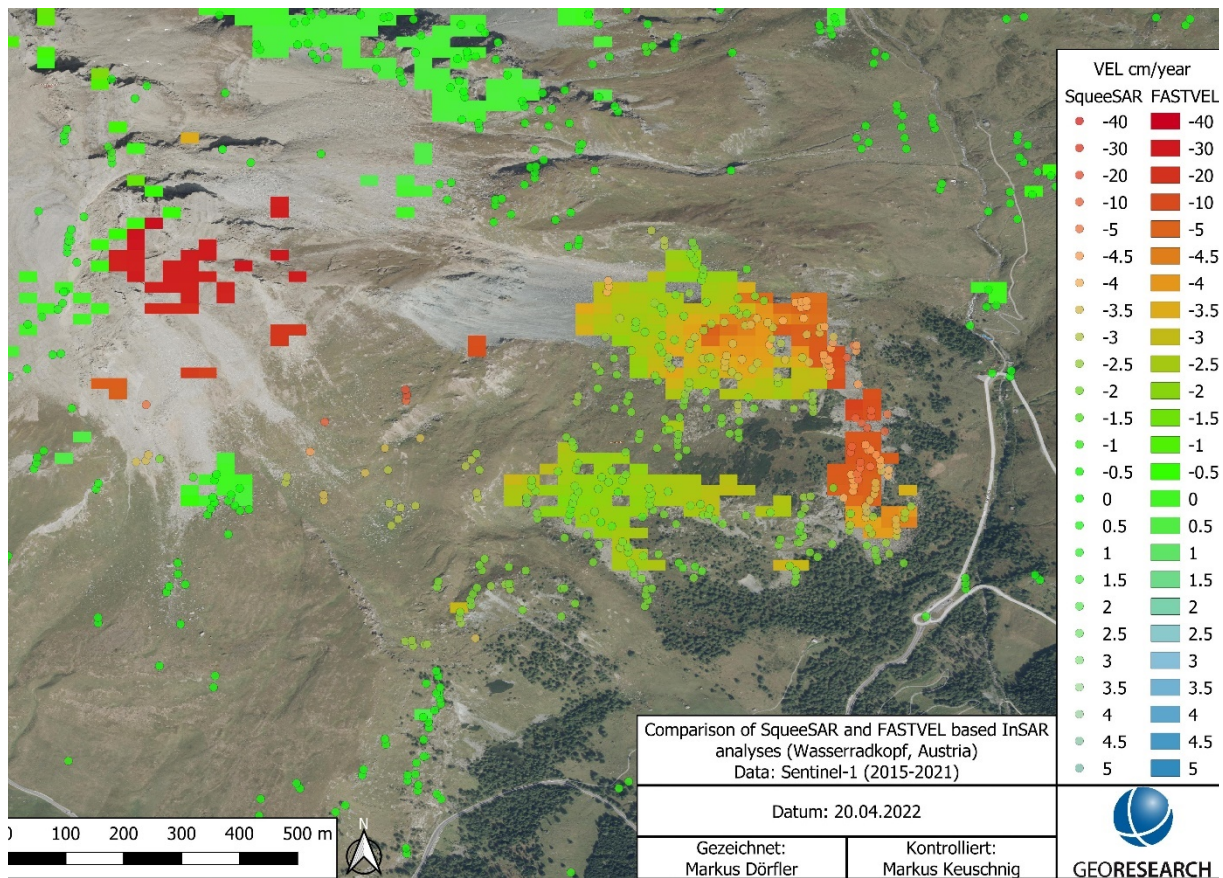


Figure 3. Comparison of results from the unwrapping algorithms SqueeSAR and FASTVEL.

The InSAR analyses carried out within the SedInOut project demonstrate the large-scale InSAR application potential in mountainous regions. As an example, a section of the Muhrtal valley (Lungau, Salzburg) is presented here, which shows a three-way division typical for the Alpine region with respect to the availability and quality of InSAR data: (i) along the valley floor, which is populated and developed with various infrastructures (roads, power lines, etc.), the data density is high, which is primarily due to the excellent radar reflectivity of man-made structures (Fig. XXa: blue zone); (ii) on the forested valley flanks, as expected, the data availability is extremely low, InSAR reflectors appear only very sporadically (Fig. XXa: green zone); (iii) in the regions above the forest line, on the

other hand, the point density is again high, which can be attributed to the favourable reflection behaviour of spatiotemporally persistent rock and debris formations (Fig. XXa: red zone).

InSAR analyses are especially very helpful for the detection of slow creep, flow, subsidence, and uplift movements. In the Muhr case study, clear surface movements are evident northeast of the Harrerspitze (see I in Fig. XXb), north of the Oblitzen (see II in Fig. XXb) and north of the Ochsenkopf (see III in Fig. XXb). As an example, Fig. XXc shows the detailed analysis of mass movement below Harrerspitze, demonstrating linear movement and a total displacement of about 100 mm for the period 2016-2020. Plots such as the displacement curve shown are excellent for illustrating the kinematics of large mass movements and demonstrate how InSAR analyses can help detect potentially dangerous accelerations of slope movements or impending sediment inputs to torrent systems at a very early stage (automatic identification of non-linear displacements).

Like slow mass movements, protective structures are also potentially well suited for InSAR-based monitoring. Assuming the absence of dense vegetation (canopy closure), larger protective structures represent adequate radar reflectors due to their persistent geometry and can accordingly be monitored over time. As an example, Figure XXb and XXd show the case of a torrent dam in the immediate vicinity of the village Vordermuhr. Over the four-year observation period (2016-2020), no significant movements were recorded, with only sporadic minor deviations occurring in the winter months due to snow cover.

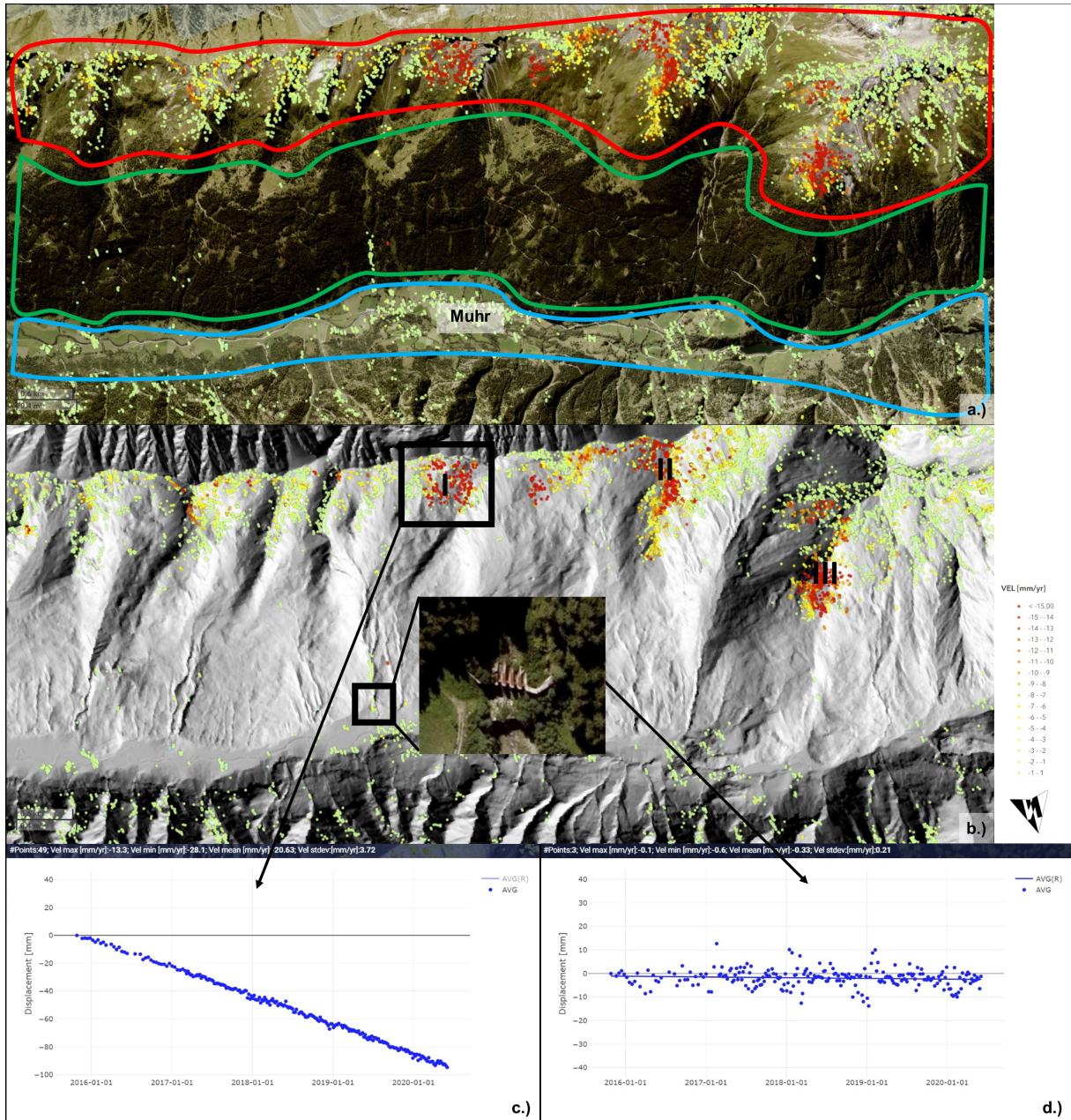


Figure 4. Case Study Muhr Municipality (Lungau, Salzburg): High InSAR point density along valley floors (buildings and infrastructures) and above the tree line (bedrock and debris).

Decision-making process

For a quick and brief overview of the different methods and the resulting products, they are summarized in Table 5. The biggest advantage of satellite data is that it is always there and available. The same is conditionally true for the ALS flights of the federal states. However, if high-resolution images are required, regardless of the type of system, there is currently no way to avoid obtaining data by helicopter or drone. The following table is a rough overview of the methods. Due to the currently increasing number of satellites, it is possible that especially the spatial and temporal resolution will change significantly in the next years. For specific feasibility questions, a remote sensing expert should be consulted in any case.

Table 5. Overview (comparison) of the different remote sensing methods.

	LIDAR	Photogrammetry	InSAR
<i>System</i>	TLS, drone, helicopter, airplane	Drone, airplane, satellite	Terrestrial, satellite
<i>System type</i>	Active	Passive	Active
<i>Sensor type</i>	Optical	Optical	Radar
<i>Wavelengths</i>	800 – 1600 nm	380 – 780 nm (visible light)	2,4 – 30 cm
<i>Spatial resolution</i>	cm – m	cm - m	cm – m
<i>Accuracy</i>	cm	cm	mm
<i>Costs</i>	\$\$	\$ - \$\$	\$\$ - \$\$\$
<i>Weather</i>	Clear visibility, day & night	Clear visibility, day	all-weather
<i>Vegetation sensitive</i>	+++	+	++
<i>Product</i>	DEM, DTM	Orthophotos, DTM	Radargram
<i>Possible analyses</i>	Volume changes	Digital Image Correlation (DIC), Object based Image Analysis (OBIA)	Deformation maps, Motion vectors, Time-series
<i>Temporal resolution of standard products</i>	Usually years	Daily - weekly	weekly
<i>Reliability</i>	+	++	+++

Final products

To make a direct comparison of the different end products, all relevant details are listed in the following table.

Table 6. Overview (comparison) of the different outcoming products from the available remote sensing methods.

	POSSIBLE SYSTEM	METHOD	APPLICATION
ORTHOPHOTO	Drone, airplane, satellite	Photogrammetry	Monitoring. early warning (only with stationary deformation camera)
DTM (DIGITAL TERRAIN MODEL)	Drone, helicopter, airplane, satellite	LIDAR, photogrammetry	Monitoring
DEM (DIGITAL ELEVATION MODEL)	Drone, helicopter, airplane, satellite (tandem missions)	LIDAR, photogrammetry	Monitoring
3D MODEL	Drone, helicopter, airplane, satellite	Photogrammetry	Monitoring
DEFORMATION MAP	Terrestrial, satellite	InSAR	Monitoring. early warning (only terrestrial)
DISPLACEMENT TIME-SERIES	Terrestrial, satellite	InSAR	Monitoring. early warning (only terrestrial)

Checklist

Requirements for decision making	Check
Size of the observation and catchment area known?	
Rough movement rate known / assumed?	
Degree of vegetation elicited?	
Time period of the active movement known?	
Purpose (monitoring / warning) known?	
Are the main final products known?	
financial resources requested?	

Draft

Determination of grain size distribution by means of photogrammetry

Focus

During the project, characteristic debris fans at the Wasserradkopf were surveyed using a UAV to subsequently examine them by means of photogrammetry regarding grain size distribution. A photogrammetry-based grain size distribution is often necessary in case the area is too exposed and conventional grain size determination methods (e.g., sieving) are not practicable. In addition, it offers the possibility to carry out these analyses without endangering man and machine.

Summary

The photogrammetric grain size analysis was carried out with the software package ShapeMetriX from 3GSM GmbH. This software package includes the Fragmenter analysis tool, which makes it possible to create grain size analyses based on drone images. At the beginning, a 3D model is created, which serves as an input file for the Fragmenter tool. After setting the evaluation parameters, the program creates a grain size analysis of the area under consideration. The evaluation can be done manually or automatically. In addition, it is also possible to carry out the analysis completely manually by drawing in the individual fragments. After the evaluation, a sieve curve is obtained, which can then be used for further purposes. For remote areas, where other possibilities to determine the grain size distribution are only available to a limited extent, the GSD determination by remote sensing techniques is a usable and practical method.

Measurement and recording techniques

The compound strategy of UAV-based data retrieval and photogrammetric processing is presented in Table 7.

Table 7. Summary of the acquisition methodology.

<p>1. Define clear objectives</p> <p>At the beginning, it is necessary to determine exactly what information is to be obtained and how the data is to be used. The way in which the data is to be used later is decisive for the required accuracy.</p>
<p>2. Flight planning Data acquisition</p> <p>Depending on the use of the data, several factors determine the achievable accuracy. In addition to effective flight planning, the selection of a suitable camera, the flight path, the weather conditions, and the UAV is of crucial importance. In principle, the accuracy achieved is linked to the ground resolution (Ground Sampling Distance, GSD) or the sampling distance. Objects smaller than the image resolution cannot be captured, and accordingly the achievable accuracy in this direction is clearly limited. (Tscharf 2020).</p> <p>Regarding the flight planning several parameters must therefore be considered. Tscharf (2020) defined the following factors:</p> <ul style="list-style-type: none"> • Flight altitude • Overlap lateral direction • Overlap longitudinal direction • Angle of view relative to the object • Control points (in case technical surveying applications) <p>Taking these points into account, Scharf 2020 makes the following recommendations for action:</p> <ul style="list-style-type: none"> • Positive effect on the accuracy achieved by image acquisition from high altitudes • High image overlap in both directions has a stabilizing effect on the image composition • An inclined orientation of the recording axis acts in a stabilizing manner • Sufficient camera movement and variation of images and acquisition positions • Combination of different factor positions increases accuracy

Further detailed information to can be found in:

Tscharf, A.: UAV-gestützte Vermessung im Bergbau – Zur Frage der Genauigkeit unter Verwendung von Structure from Motion, Diss., Leoben, Montanuniv., Lehrst. F. Bergbaukunde, Bergtechnik und Bergwirtschaft, 2020. <https://doi.org/10.1007/s00501-020-00988-x>

3. Software-supported data evaluation

The photogrammetric analysis described here is carried out with the software package ShapeMetriX (Fragmenter Tool) from the company 3GSM GmbH (<https://3gsm.at/de/produkte/bmx-fragmenter/>).

This makes it possible to create grain size analyses based on drone images. At the beginning, a 3D model is created, which serves as an input file for the Fragmenter Tool. After setting the evaluation parameters, the program creates a 3D grain size analysis of the area under consideration. The analysis can be carried out manually or automatically. There are two modes for automated evaluation, "RipRap" and "Blast". According to the provider, the "Blast" mode is suitable for heterogeneously distributed grain sizes and the "RipRap" mode for homogeneously distributed grain size compositions. These software-based and automatically generated analyses can then be post-processed manually. In addition, it is also possible to carry out the analysis completely manually by drawing in the individual fragments. After the algorithm of the software has evaluated the data, a sieving curve is obtained, which can then be used for further applications.

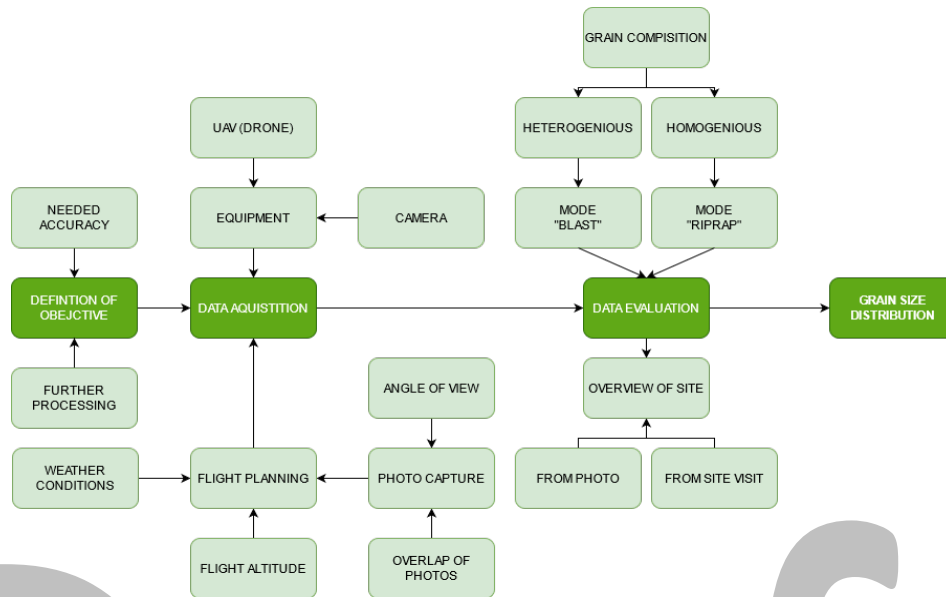


Figure 5. Sketch of the acquisition methodology, determining the grain size distribution of debris compartments.

The output is finally a detailed sieving curve and a statistical evaluation. Within the 3D Modell the varied sizes of the grains are displayed in assorted colors which can help to interpret the model. It must be noted that in general, optical UAV-based analysis methods can only detect what they capture on the surface. As the rock fragments of debris fans are often directional positioned, it is possible that sections of the individual fragments are thus partially covered. Therefore, photogrammetry-based analysis could show an underestimation of the GSD. Furthermore, UAV-based methods do not provide any information about the composition at depth. Therefore, a first impression should be made together with the evaluation, at least on site or based on photos, to ensure that the results are reliable.

Decision making progress

UAV-based grain size analyses are practicable and offer an efficient alternative to traditional grain size determinations with limitations. These limitations are, for example, that no information is obtained about the grain size distribution at depth. Especially for remote or exposed areas, where grain size analysis is not possible, UAV-based grain size analysis offers a great alternative.

Example

As an example, a debris fan at the Wasserradkopf was surveyed with a drone to subsequently examine them by means of photogrammetry regarding grain size distribution (GSD) as described in the previous parts. The photogrammetric analysis was carried out with the software package ShapeMetriX from 3GSM GmbH (<https://3gsm.at/de/kontakte/>). This software package includes the Fragmenter analysis tool. This makes it possible to create grain size analyses based on drone images. At the beginning, a 3D model is created, which serves as an input file for the Fragmenter tool (<https://3gsm.at/de/produkte/bmx-fragmenter/>). After setting the evaluation parameters, the program creates a grain size analysis of the area under consideration.

There are various setting options within the program. The evaluation can be done manually or automatically. In the automated evaluation option, there are two modes, "RipRap" and "Blast". According to the developer, the "Blast" mode is suitable for heterogeneously distributed grain sizes and the "RipRap" mode for homogeneously distributed grain size compositions. These software-based and automatically generated analyses can be manually post-processed afterwards. In addition, it is also possible to carry out the analysis completely manually by drawing in the individual fragments.

To compare the accuracy of the individual evaluation modes, representative areas (were mapped manually. For this purpose, 10x10 m nets were placed on the debris fan and rock samples were measured every 50 cm (in x and y direction). These results were then digitized.



Figure 6. Overview of the debris fan at the study site Wasserradkopf.



Figure 7. Measurement grid installed within the modelled area.

The comparison (Figure 8) of the herein presented area shows a high degree of conformity for the on-site measured grain sizes with the automated determination mode "RipRap", while the automatic evaluation "Blast" mode seems to underestimate the grain sizes (a GSD measured on site is taken as a reference). The on-site inspection shows a homogeneous grain size distribution, which might be the reason that the automatic determination mode "RipRap" (recommended mode for homogeneous grain – size distributions) provides the best results.

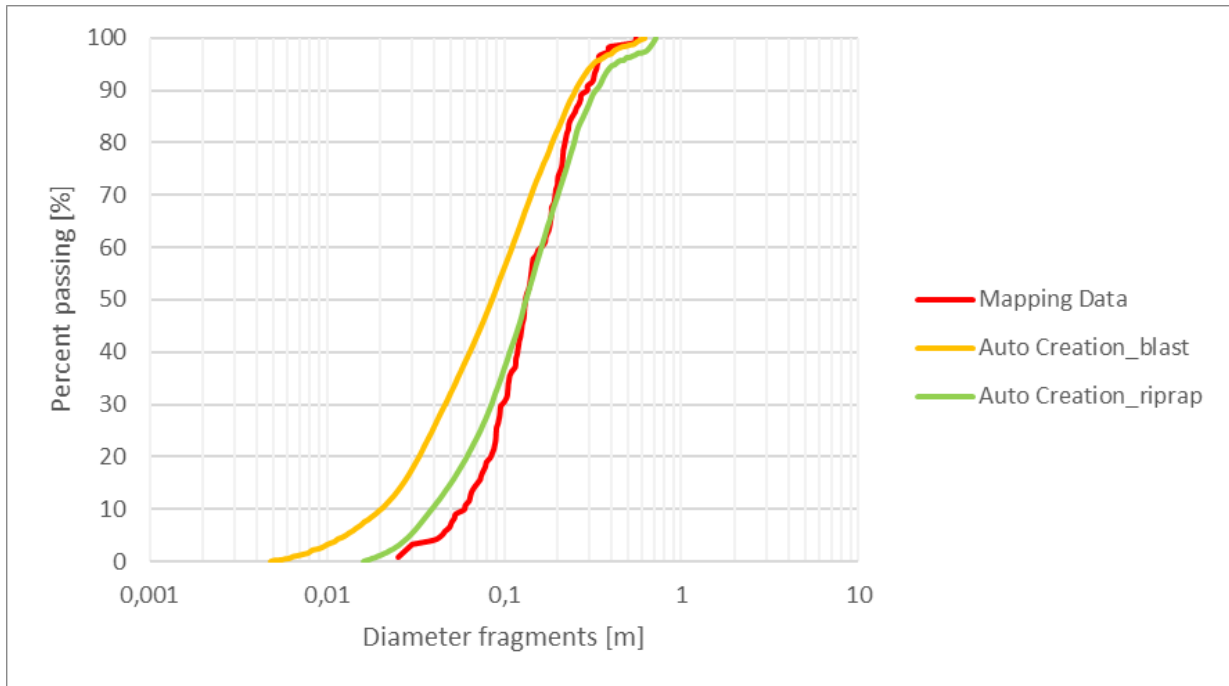


Figure 8. Comparison of data in model domain.

As the rock fragments of debris fans are often directional positioned, it is possible that sections of the individual fragments are thus partially covered. Therefore, photogrammetry-based GSD analysis might show an underestimation of the particle sizes. The result of the area presented here also shows an underestimation of the particle sizes, which may be explained by the effect of coverage. In addition, in debris fans (especially in heterogeneous areas) smaller particles are detected by the software, whereas in the applied method (manual measurement of the individual particles) they remain undetected, since the fines spatially not uniform contributed. Taking this into consideration, the fine proportion would increase and thus the GSD curves would be brought closer together and an even higher level of conformity would be achieved.

Geomorphological analysis

Focus

The assessment of solid volumes that are prone for mobilisation in a debris flow basin requires an innovative geomorphological approach. Thereby, the method is based on the photo-interpretative analysis of aerial photographs, orthophotos and products derived from high-resolution digital terrain models (e.g., shaded relief maps, slope, surface roughness). Further, ground investigations aim at the identification and classification of sediment sources, while guaranteeing both accurate mapping and the quantification of their potential contribution to debris flows. These debris flow contributions concern torrential riverbeds, unstable or eroding banks and landslides, that are directly connected to the drainage network. All these parameters are listed in a standardised survey sheet, capturing the spatial and temporal distribution of debris-flow events.

Summary

The preparation of a sediment source area inventory is detrimental to document the extent of slope downwasting within a catchment. Additionally, it is required to assess the distribution, types, trends, recurrence, and statistics of slope instabilities. The determination of process-related risk susceptibility, vulnerability and hazard potential associated with mass wasting processes ensures the high-quality standards of the inventory (Guzzetti et al., 2012).

The mapping and proper classification of sediment source areas counts as a fundamental prerequisite for the assessment of potentially mobilizable volumes in each catchment. Such inventories can be prepared while addressing different objectives such as the purpose of the inventory, the extent of the study area, the scale of the base topography, the resolution and characteristics of the available images and the experience of the operator (van Westen et al., 2006; Guzzetti et al., 2012). The traditional (most widespread) way of mapping instabilities is based on the interpretation of aerial photos, orthophotos and DTM-derived products, typically carried out in a GIS environment.

In this regard, this manual refers to the works of Brardinoni et al. (2003); Brardinoni et al. (2009) and Guzzetti et al. (2012) that provide useful indications on the production of accurate landslide

inventories and the analysis of their attributes. As mentioned above, the results of the photo-interpretative analysis should be supplemented with ground surveys also aimed at validating the inventories produced in a GIS-environment.

The SedInOut project targets the definition of a standardised data acquisition methodology for sediment source areas. For this reason, the scientific partners developed a field survey sheet. This sheet, which in part takes its cue from a sheet developed within the European project SedAlp (Brardinoni and Cavalli, 2012), is described in the following section, while representing the guidelines for its compilation.

Measurement and recording methodologies

Guidelines for the use of the survey sheet

This manual aims to define the drafting methodology of the survey sheet of sediment source areas and their transport in a high-mountain environment.

The sheet stems from the need to accompany the professional in surveying the terrain and helping him/her to standardise and categorise the descriptive information necessary for a correct cataloguing of data.

Structure

The attached survey sheet is divided into four sections:

- ✓ Main characteristics
- ✓ Material and texture
- ✓ Geometry
- ✓ Sediment transport

Definition of sediment source areas

A sediment source area is defined as an area characterised by the presence of sediment. The area is characterised by the occurrence of high-intensity erosional and/or instability processes. Sediment source areas undergoing erosion (= detachment, transport and deposition of soil or sediment due to wind, rain impact or water runoff) and hold a potential volume of transportable

sediment. The detail of classification of sediment source areas depends on the purpose of the study. It is advisable to make a circumspect and specific compilation of the study areas in the field sheets, as simplification and grouping are possible in phases of subsequent analysis.

Main characteristics

Typology

The different types of movement have been summarised as follows: sliding, flow, avalanche, collapse, and soil erosion.

The two main types of landslides by sliding are defined as rotational and translational (Figure 9).

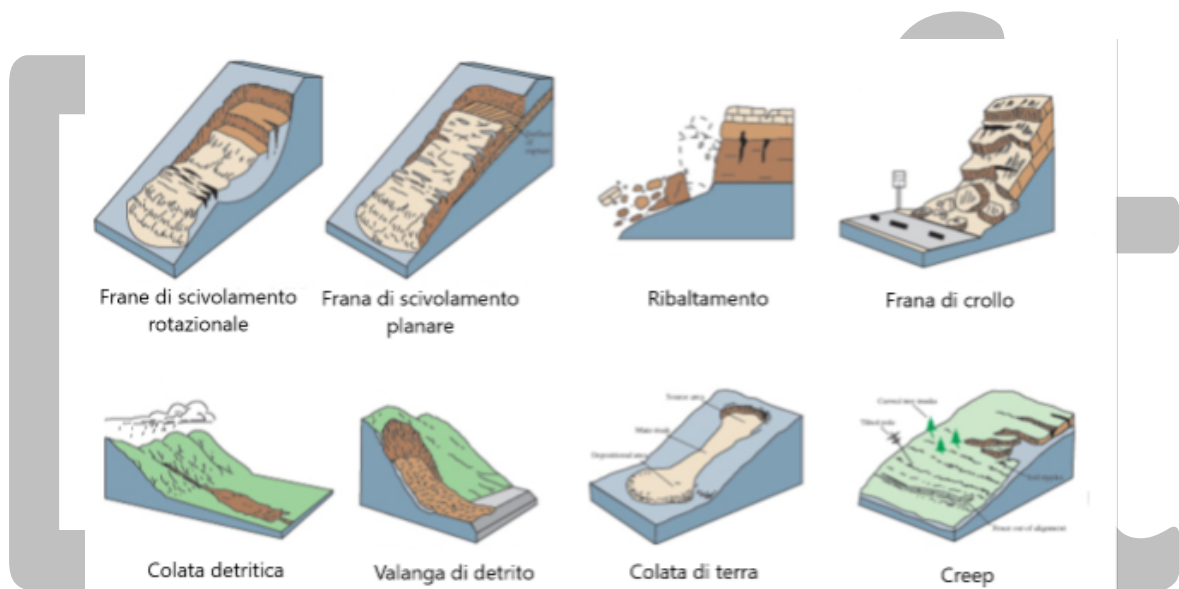


Figure 9. Combination of the different types of mass movements (modified from US Geological Survey, 2004).

Land cover

This section indicates the type of ground cover, which has been divided into: E: Herbaceous cover, C: Shrubs, A: Trees, SN: Bare soil.

Vegetation plays a fundamental role in the study of the hazard of natural phenomena as the root system generates a stabilising effect against landslide and surface erosion phenomena.

Location of the source area

Depending on the proper location of the sediment source area, the following categories are distinguished: OS: Open Slope, S: Escarpment, TC: Channel Head, SC: Channel Banks, C: Channel, ES: Bank Erosion, RG: Rock Glacier Front and DM: Moraine Ridge.

Sources/runoff

Please indicate whether there are any springs or runoff within the sediment source area (yes/no).

Adjusted depth

The regolith originates from the degradation of bedrock due to the erosive activity of exogenous agents and organic activity (Figure 10).

It is recommended to indicate the depth of the regolith. It may be absent or may extend up to hundreds of metres.

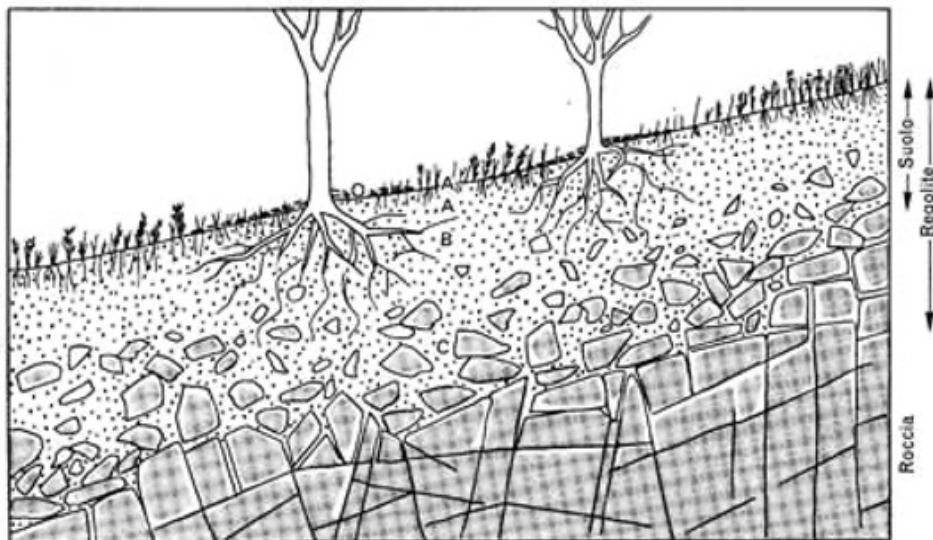


Figure 10. Simplified scheme for the identification of regolith (Castiglioni, 1996).

Bedrock

Indicate whether the bedrock is outcropping and, if so, whether it is (Figure 11)

M: Massive,

S: Stratified,

C: Cataclastic

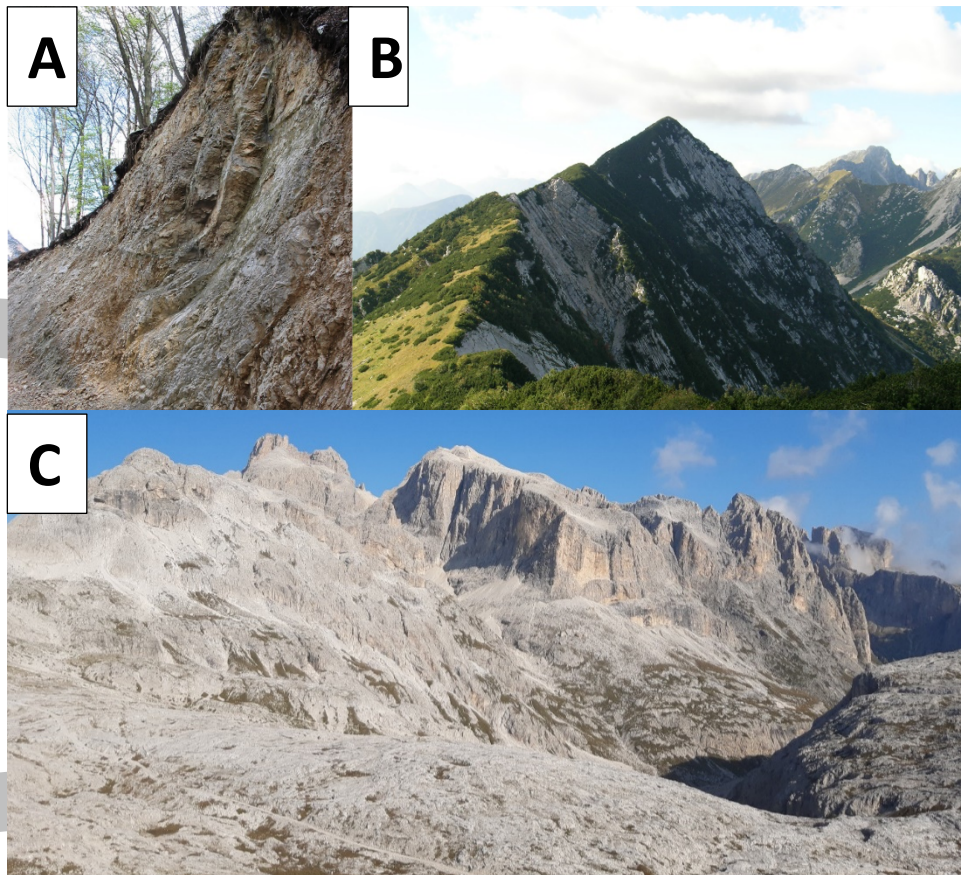


Figure 11. A) intensely fractured and cataclastic dolomitic rock mass; B) well stratified rock mass; C) massive rock mass. (Pale di San Martino, Western Dolomites).

Materials and texture

Type

Indicate the material constituting the sediment source area from the following: A: Clay, S: Silt, SA: Sand, G: Gravel, C: Pebbles (64-128 mm), B: Blocks (128-258 mm), D: Diamicton (Figure 12).

Diamicton is a type of poorly sorted sediment of terrigenous origin containing particles of variable size, from clay to boulder, embedded in a matrix. This term is purely textural and has no genetic attribution.

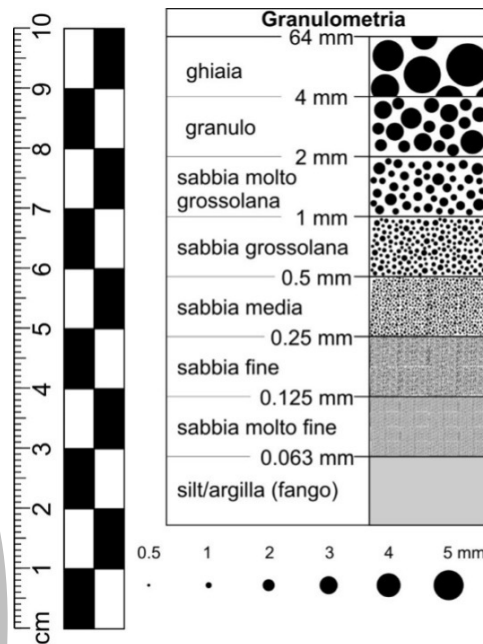


Figure 12. Diagram for visual grain size estimation, centred on sand classes (Graphic: Samuele Papeschi).

Texture

Indicate the texture of the sediment source area between: SM: Matrix-bearing, SC: Clastic bearing, DS: Loose deposit, PS: Partially loose (Figure 13).

- Deposits are *matrix-supported* when they are not in contact with each other and are immersed within a mixture of fine material (silt, clay, and organic material).
- Deposits are *clast-supported* when the coarse part of the deposit is in contact (stable deposit).
- Deposits are (*partially*) *loose* when there is a lack of matrix and stability.

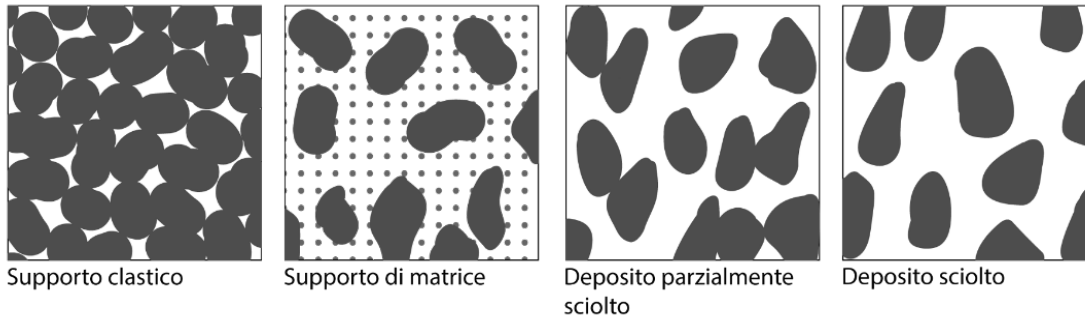


Figure 13. Graphical representation of the different types of support.

Genesis

Indicate the origin of the deposit between: T: Till, C: Colluvium, D: Debris flow deposit, Ta: Talus.

- The term *till* identifies a glacialic, generally matrix-supported, poorly sorted deposit with subrounded clasts. Sometimes the clasts may represent striations.
- *Colluvium* represents a deposit transported predominantly by the action of gravity and surface runoff, generally containing silt, cobble sand and generally angular or sub-angular boulders.
- *Debris flow deposits* are characterized by a large amount of chaotic, coarse sediment recognizable in fronts and tongues with convex morphology. It is a process involving sediment and water driven mainly by the quantity and availability of loose sediment and gravity.
- *Talus* are gravity deposits composed mainly of sandy-gravel material found at the foot of vertical/sub-vertical rock faces.

Geometry

The following parameters need to be captured:

- 1- Slope height at head
- 2- Average height of side slopes
- 3- Length
- 4- Average width

- 5- Cross section
- 6- Longitudinal profile
- 7- Slope of trigger zone
- 8- Slope of transport zone
- 9- Slope of deposition zone

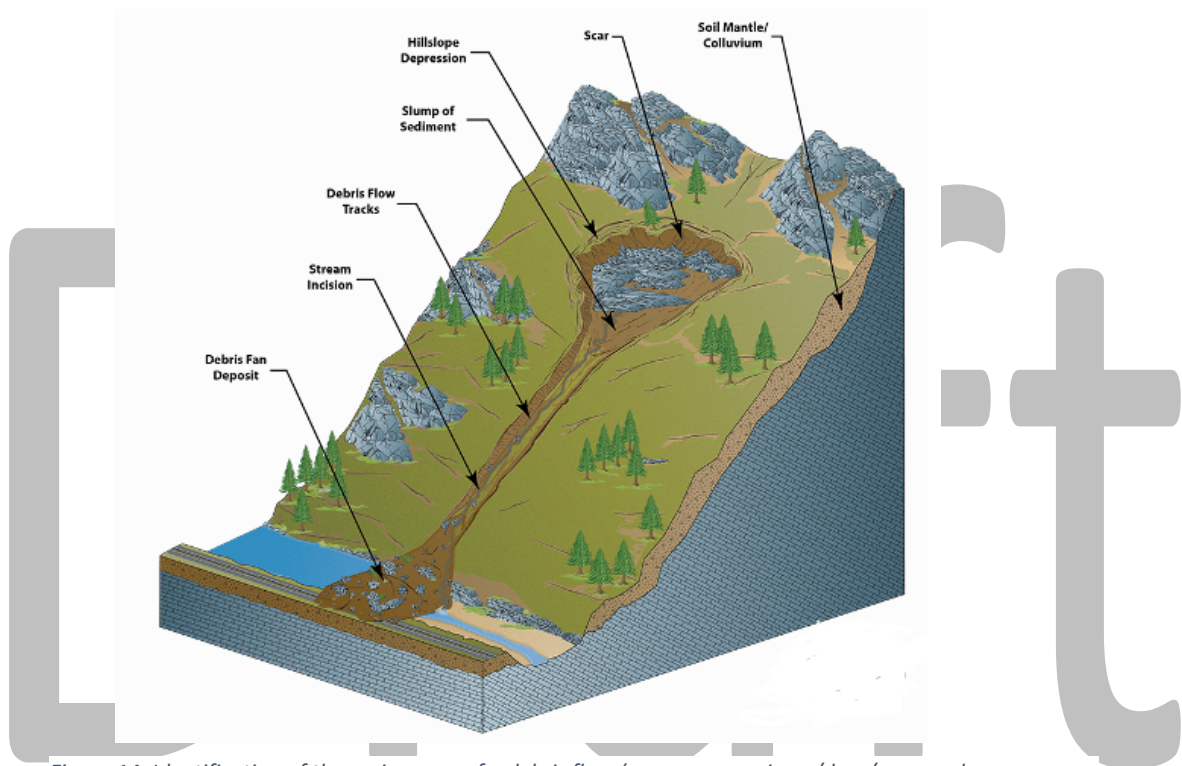


Figure 14. Identification of the main zones of a debris flow (www.wsgs.wyi.gov/docs/wsgs-web-landslides.pdf); below, nomenclature of the main shapes of a landslide (Varnes, 1978).

Sediment transport potential

The sediment delivery potential refers to the ability of a given source area to convey sediment downstream. Since the amount of sediment that can be transported is site-specific (depends on rainfall regime, rock substrate type, soil depth, etc.) it is necessary to recognize erosion areas with a high sediment delivery potential.

In total, four main cases of conveyance need to be distinguished:

- 1- the generated sediment is not able to be mobilized. The sediment remains stored within the sediment source area
- 2- the sediment source area is connected to a tributary channel tributary. It is unlikely that this sediment will reach the valley bottom (exception: long time lag)
- 3- the sediment source area is connected to a tributary channel and has a medium-high delivery potential (the stored sediment will be able to reach the valley bottom)
- 4- the sediment is directly connected to the valley bottom (high potential, Figure 15).

The sediment delivery potential must be indicated according to the following four classes:

- 1- Low (in situ),
- 2- Medium-low (rock channel - colluvial),
- 3- Medium-high (tributary channel - semi alluvial),
- 4- High (main channel - alluvial) (Fig. 15).

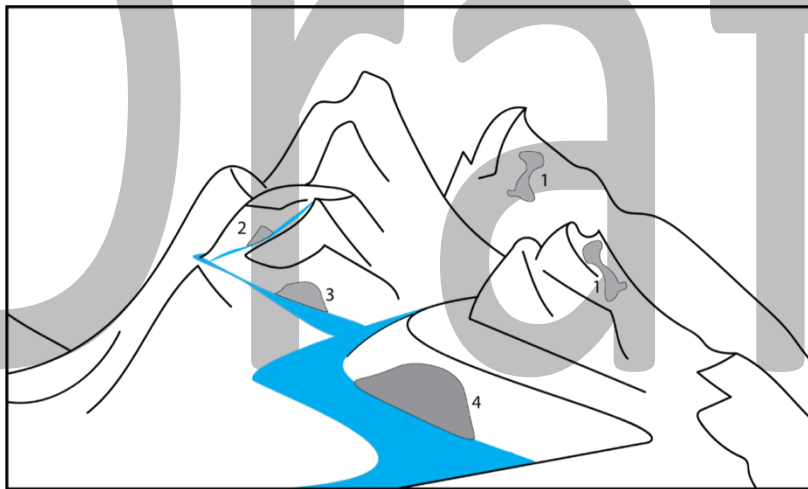


Figure 15. Example diagram to recognise the different connection potential of the sediment. 1: low potential - in situ, 2: medium-low potential (rock channel - colluvial), 3: medium-high potential (tributary channel - semi alluvial), 4: high potential (main channel).

Obstacles

Indicate the possible obstacles to sediment flow between (Figure 16):

- 1: Suspended valley
- 2: Moraine,
- 3: Glacier,
- 4: Rock glacier,
- 5: Deposit,
- 6: Cone,
- 7: River terrace,
- 8: Flood plain,
- 9: Lake (Fig. 16),
- 10: Dams/weirs,
- 11: Containment works,
- 12: Roads/infrastructure.



Figure 16. Example of sediment dislocation caused by a pond in a suspended valley in a dolomitic environment. (Upper part of the Giralba torrent basin, Belluno Dolomites).

Final products



Figure 17. Surface landslide along the banks of a secondary stream with outcropping bedrock.

Nome bacino: Rio Buscagna		ID bacino: Rbu	Data: 02/07/2022																			
ID	Codice identificativo	Caratteristiche principali				Materiale e tessitura				Geomorfologia				Accoppiamento sedimenti								
		Tipologia (1)	Copertura suolo (4)	Localizzazione e dell'area sorgente (3)	Sorgimento (4)	Profondità regole (m)	Bedrock (5)	Tipo (6)	Tessitura (7)	Genesi (8)	Altezza scarpata in testata (m)	Altezza media scarpata laterali (m)	Lunghezza (m)	Larghezza media (m)	Sezione trasversale (9)	Profilo longitudinale (10)	Pendenza zona innesco (1)	Pendenza zona di trasporto (1)	Pendenza zona di deposizione (1)	Potenziale (11)	Ostacoli (12)	
1	Rbu_01	1	SW	SC	N	0.5	C	D	DS	C	0.5	0.2	5	2	CC	L	SB	45	35	3	-	
2																						
3																						
4																						
5																						
6																						
7																						
8																						
9																						
10																						
11																						
12																						
13																						
14																						
15																						
16																						
17																						
18																						
19																						
20																						

1. Scioglimento	3. OS: Open Slope	6. A: Argilla	9. L: Lineare	11. Basso (in situ)
2. Flusso	4. SC: Scarpata	7. SM: Supporto di matrice	10. C: Concavo	12. Medio-basso (canale in roccia - colluviale)
3. Valanga	5. SI: Sponde di canale	8. SC: Supporto clastico	11. CV: Convesso	13. Medio-alto (canale tributario - semi-alluvionale)
4. Crollo	6. CA: Canale	9. DS: deposito sciolto	12. CM: Complesso	14. Alto (canale principale - alluvionale)
5. Erosione	7. ES: Emissione di sponda	10. D: Diamotoni	13. L: Lineare	15. Valle scoscesa
6. Copertura erbacea	8. FR: Fronte di Rocce glaciali	11. B: Blocchi	14. C: Concavo	16. Moenae
7. Cespugli	9. DM: Dorzale morenica	12. D: Diamotoni	15. CV: Convesso	17. Rock glacier
8. Alberi		13. PS: Parzialmente sciolto	16. CM: Complesso	18. Deposito
9. Suolo nudo				19. Conoide
				20. Terrazzo fluviale
				21. Piana Alluvionale
				22. Lago
				23. Dighe/bastie
				24. Opere di contenimento
				25. Strade/Infrastrutture

Note	
Rbu_01: il materiale rilasciato dall'area sorgente raggiunge facilmente il corso d'acqua	

Figure 18. Excel file Sediment compilation survey sheet.

Decision-making progress: Guideline for identifying debris flows

The distinction between debris flows and floods with solid transport is essentially based on differences in solid concentration (much higher in the case of debris flows), followed by variances in overall rheological behaviour. In debris flows, water and solids move with the same velocity, whereas in floods with solid transport, the sediment transported to the bottom has a different velocity from that of the water with suspended sediment in which it is immersed.

An important element that differentiates debris flows from many types of landslides is the fact that many landslides (partially) preserve the initial structure of the material affected by the movement. This is not the case for debris flows: the flowing mass undergoes strong deformations, to the point of being completely remodelled. This difference is lessened if one compares debris flows and rock avalanches (rock avalanche and debris avalanche), which differ in the different role played by water. While the dynamics of rock and debris avalanches are controlled by the interactions between solid particles, in debris avalanches both the forces acting on the solid fraction and those affecting the liquid component intervene. The correct recognition of the process is vital for the determination of the hazard and for the selection of the most appropriate risk mitigation measures.

An example of the approach that frames debris flows in a broader spectrum ranging from water currents to landslides is provided by Coussot and Meunier's (1996) classification (Figure), where in addition to the concentration of solids, the role of the granulometric characteristics of the materials involved is considered, distinguishing between cohesive and granular materials.

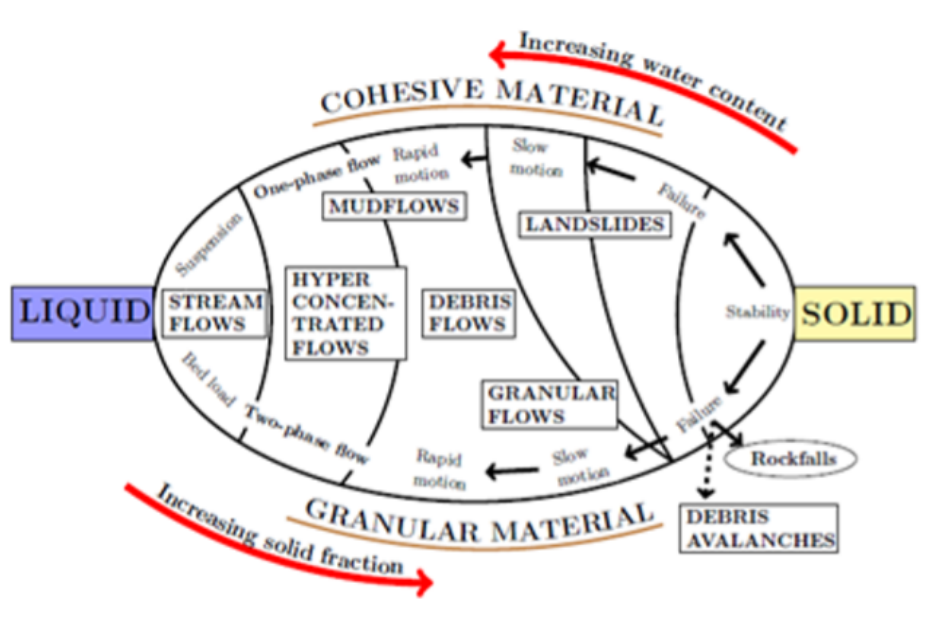


Figure 19. Classification of mass movements on steeply sloping surfaces (modified from Coussot and Meunier, 1996).

Draft

Evaluation of remobilization of sediment (debris fans)

Focus

Sediment deposits (e.g., debris fans) often contain enormous quantities of sediment in a fragile equilibrium. External influences such as extreme weather events, rockfalls, or seismicity can disturb the equilibrium of these sediment accumulations. By modeling debris fans numerically and simulating external influences with varying intensities, the stability of debris fans can be determined and conclusions regarding the hazard potential can be drawn.

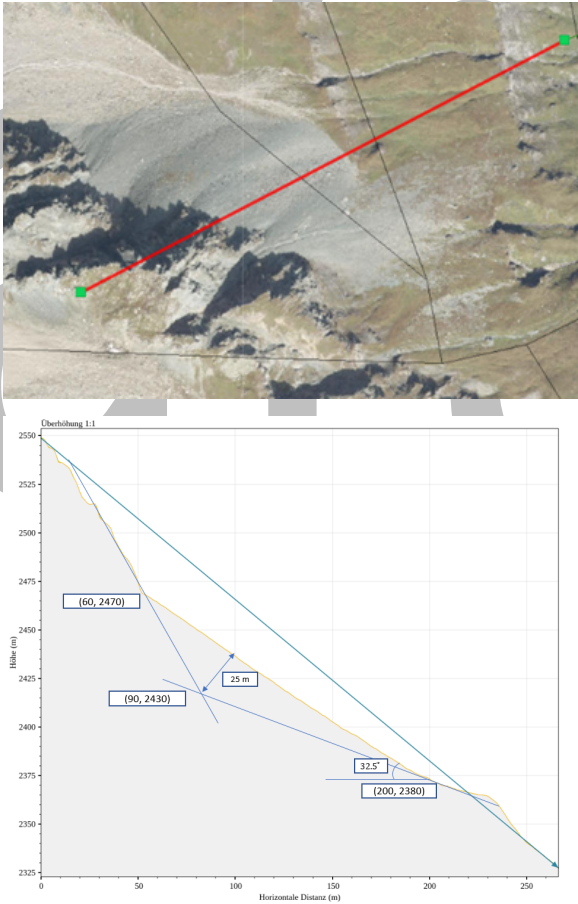
Summary

For the determination of the hazard potential of a debris fan, the software PFC2D (<https://www.itascacg.com/software/PFC>) is used. It allows to simulate the behavior of debris fans under a wide range of conditions. The discrete system of PFC2D, which consists of regular or irregular particles, can simulate the interaction between the grains. The particles interact through normal and shear springs that can translate, rotate, and change position according to the forces and moments acting on the center of the particles. The particles can be bound or unbound using contact models, simulating linear elastic behavior. Thus, with some simplifications, it is possible to get a first impression of the stability of debris accumulations.

Measurement and recording techniques

The compound strategy of hazard potential modelling is presented in Table.

<p>Model generation</p>	<p>In the simulation software, the particles are usually disk-shaped in 2D models and spherical in 3D models. To simulate the irregular geometries of the debris fan, disk-shaped and spherical particles cannot meet the geometric requirements. Therefore, clumps are used. A single clump is a rigid collection of disk- or spherical-shaped particles and can therefore describe an individual shape of a particle based on any template. Clumps can be a suitable representative for debris fans since they can move, rotate, and obey the equations of motion. Moreover, the surface properties of a clump can be specified independently for each particle.</p>
<p>Grain size distribution and shape of particles</p>	<p>To begin the particle size and distribution must be selected. For this purpose, the GSD of the debris fan is used as input. After determining the particle size and its percentage, the geometry of each particle is drawn with a CAD program, according to the particle shape of samples or photos of the debris fan. Then, the geometry is imported into the software to create the clump template. Finally, the particle distribution can</p>

	<p>be prepared according to the percentage of particles.</p>
<p>Modelling of the area under investigation</p>	<p>To determine the geometry of the debris fan, GIS software must be used. First, a cross section in the longitudinal direction of the debris fan is created. Second, a line parallel to the largest slope and a line parallel to the smallest slope must be constructed to obtain information about the thickness of the debris fan. By intersecting these two lines, the thickness of the debris fan as well as its depth limit can be estimated (Figure 20).</p>  <p><i>Figure 20. Determination of the geometry of the slope.</i></p>

	<p>The next step is to export the simulated particles to slope to create final model.</p>
<p>Selection of micro parameters and scaling</p>	<p>Information on the limit state of the debris fan is obtained by using the "trial and error" method in combination with literature. By using different values for the micro parameters (porosity, density, friction coefficient, shear stiffness, damping) the limit state is evaluated. In addition, a linear elastic model is assumed with no bonding or cementation between particles. The model itself is controlled by elastic and friction behaviour.</p> <p>To speed up the computation time, the individual particles can be scaled up.</p>
<p>Hazard modelling</p>	<p>Since the debris fan is modelled, the response of the stable model to potential hazards such block falling (rock fall), water flow (Rainfall), and seismic events can be analyzed.</p>
<p>Rock fall</p>	<p>Initially, the block to be simulated is drawn with CAD and embedded in the software. Depending on the scale factor for the individual particles of the debris fan, this block should also have the corresponding scale factor. After that, the location from where the block starts to fall is determined. The falling block has no velocity at the beginning and is accelerated by gravity. The software then allows the evaluation of the maximum deflection of the debris fan caused by the impact of the block.</p>

Rainfall	To simulate the water flow, Darcy's law must be used to calculate the pressure acting on each particle inside the debris fan. This is done as a function of the maximum amount of precipitation measured in the studied area. In this way, stability can be determined for a wide range of precipitation amounts. It is advisable to use higher values than those measured to model a particular channel formation.
Seismicity	To model seismic activity, the maximum horizontal reference ground acceleration must first be determined. This horizontal acceleration is then applied to the model. Subsequently, the stability can be evaluated for different intensities.

Final products

A numerical stability analysis of debris fans allows predictions of how resistant and sensitive they are to external influences such as extreme weather events, rockfalls and seismicity. This provides the opportunity to develop different scenarios and determine what intensity these external influences require to lead to large-scale remobilization. With this knowledge, preventive measures can be taken in advance. It must be added that the methods presented contain some simplifications. For example, the modeling assumes a heterogeneous grain size distribution throughout the debris fan. Therefore, the numerical models must be paired and interpreted with experience and, if necessary, verified by in-depth numerical simulations and experiments.

Decision-making progress

Numerical modeling (and stability analysis) of debris fans is an opportunity to understand processes leading to remobilization. They also provide an opportunity to study in more detail the intensity of external influences that lead to remobilization. Numerical modeling is therefore

particularly useful for debris fans posing a risk to people or infrastructure, and for describing that risk qualitatively. They offer the possibility to obtain initial indications and to investigate them in more detail, if necessary.

Example

During the project, a debris fan at the Wasserradkopf in Carinthia was investigated for its stability. The photogrammetrically determined GSD (cf. chapter Photogrammetry) was used as input parameters and divided into 4 representative groups (Table 8).

Table 8. The GSD divided into four groups.

Particle size (m) and Percentage (%)
0.001 < 20% < 0.21
0.21 < 30% < 0.38
0.38 < 20% < 0.63
0.63 < 30% < 0.7

After determining the particle size and its percentage, the geometry of the particles is constructed using AutoCAD according to the detail photos of each particle. Then, the geometry is imported into PFC2D to create the clump templates (Figure 21)



Figure 21. Examples of the created lumps templates.

Depending on the percentages of particles in the clump templates, the particle distributions can then be arranged.

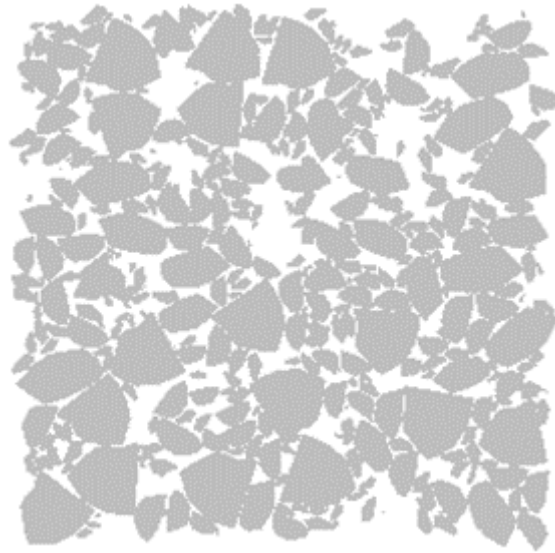


Figure 22. The final particle distribution used for the model.

To determine the geometry of the debris fan, a cross section is constructed in the longitudinal direction of the debris fan. To obtain information about the thickness of the debris fan, a line parallel to the largest slope and a line parallel to the smallest slope were constructed. By intersecting these two lines, it is possible to estimate the thickness of the debris fan as well as its boundary in depth (Figure 23). Figure 23 shows that the thickest part of the debris fan is about 25 meters, and the length and height are 140 and 120 meters, respectively.

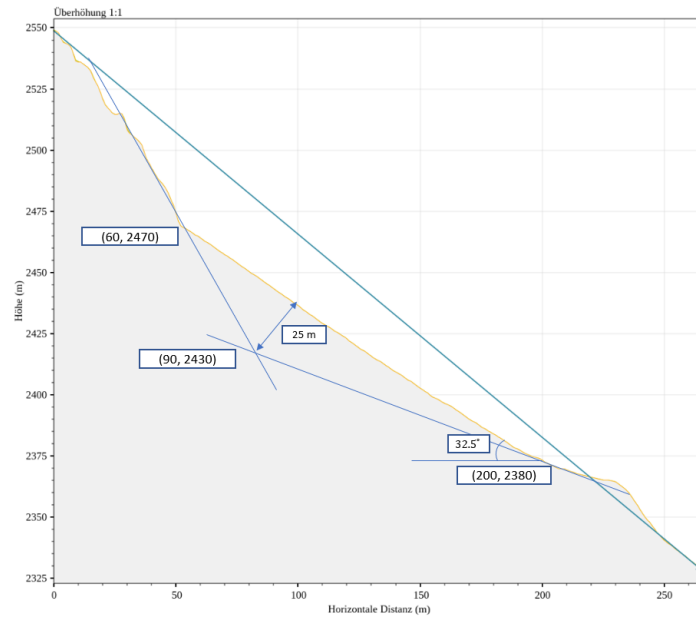


Figure 23. Example for the determination of the thickness of a debris fan.

The next step was to import all simulated particles into the slope to create the final model (Figure 24). According to the extracted geometry, the limiting angle of the debris fan is about 32.5°. To achieve this angle, experience from the literature was combined with "trial and error". By varying the values for the micro-parameters, the limit state boundaries for the numerical simulation could be found out (Table 9). To speed up the computation time, an upscaling by a factor of 5 was applied. In the model itself, a linear elastic model is used, and no bonding or cementation between particles is considered. In addition, the model is controlled by elastic and frictional behaviour.

Table 9. Chosen micro parameters for the numerical model.

Micro parameters of linear model	
Porosity (%)	8
Density ($\frac{kg}{m^3}$)	2500
Friction coefficient (μ)	0.5
Normal to shear stiffness ($\frac{k_n}{k_s}$)	1
Damping	0.3

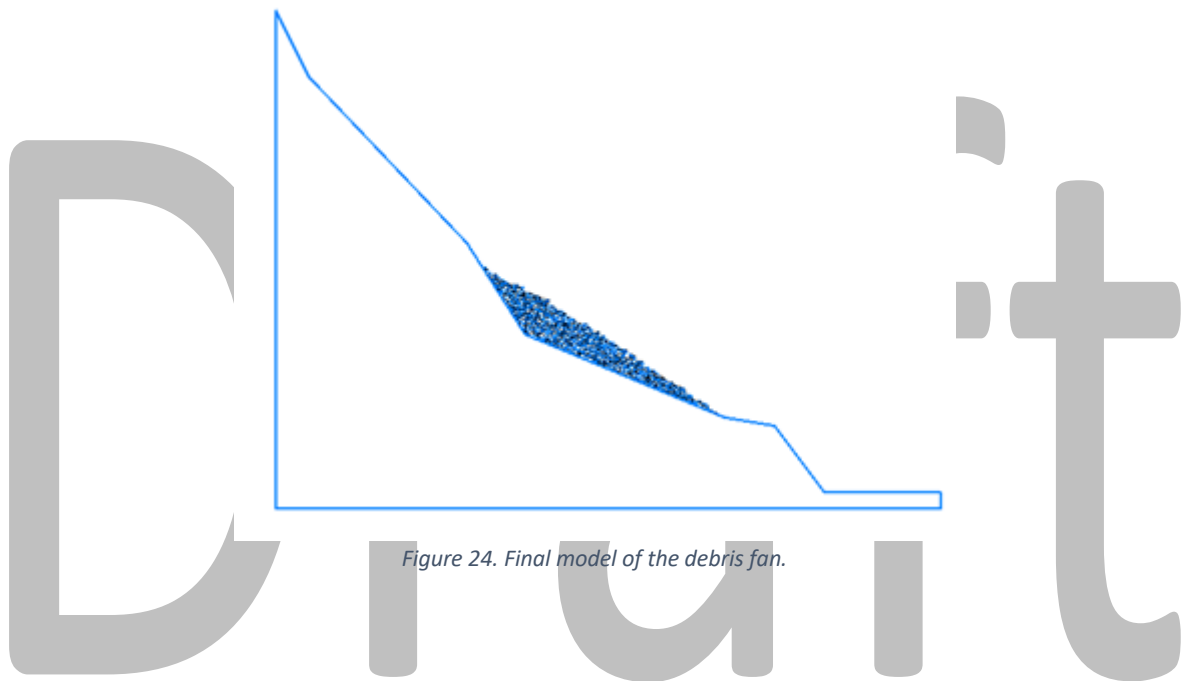


Figure 24. Final model of the debris fan.

The investigation of potential hazards is one of the main objectives. After simulating the debris fan, the response of the stable model to potential hazards such as rockfall, extreme weather events, and seismicity was comprehensively analyzed. For a potential rockfall on the debris fan, the falling block to be simulated was drawn with CAD and embedded in the PFC software. Depending on the scaling factor, the individual particles of the debris fan have the same scaling factor. In this case, a scaling factor of 6 was chosen. Next, the location from which the block starts to fall is determined. The falling block has no velocity at the beginning and is accelerated by gravity. The software then allows the evaluation of the maximum deflection of the debris fan induced by the impact of the block (Figure 25).

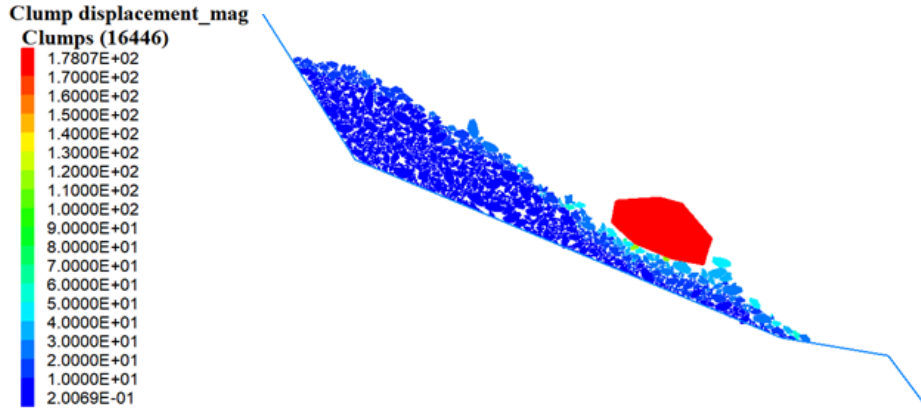


Figure 25. The maximum displacement and location of the block after the impact on the debris fan.

To simulate extreme weather events, Darcy's law was used to calculate the pressure inside the debris fan. The maximum measured precipitation monitored in the area was used as the input value. The force exerted by the water on the particles was determined from the pressure value of 123.3 N/m^2 . Since there were four distinct groups of particles in this study, the area of each group was used to calculate the equivalent force. Finally, the obtained forces are applied to the model in the downslope direction to simulate the water flow, and the displacements induced can be simulated (Figure 26).

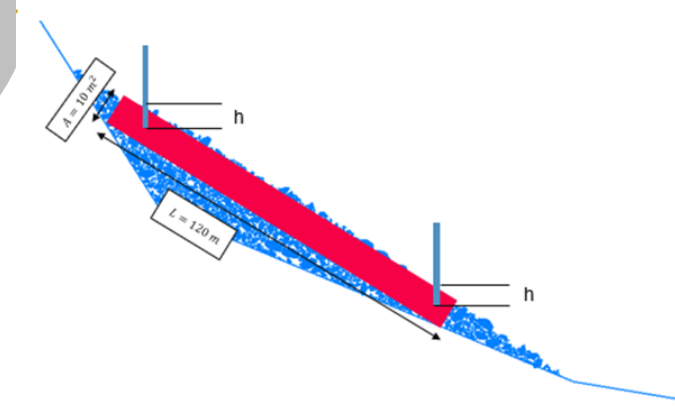


Figure 26. Darcy's law is applied to the debris fan.

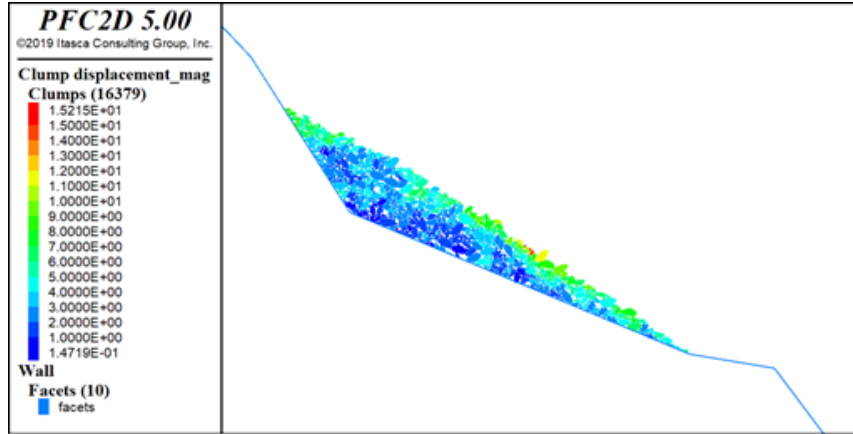


Figure 27. Displacements of the debris fan triggered by water flow.

To simulate seismicity, horizontal acceleration was applied to the model. For this purpose, the maximum measured horizontal acceleration for the project area was determined and therefore the value of 0.5 m/s² was selected. The Results can be found in Figure 28.

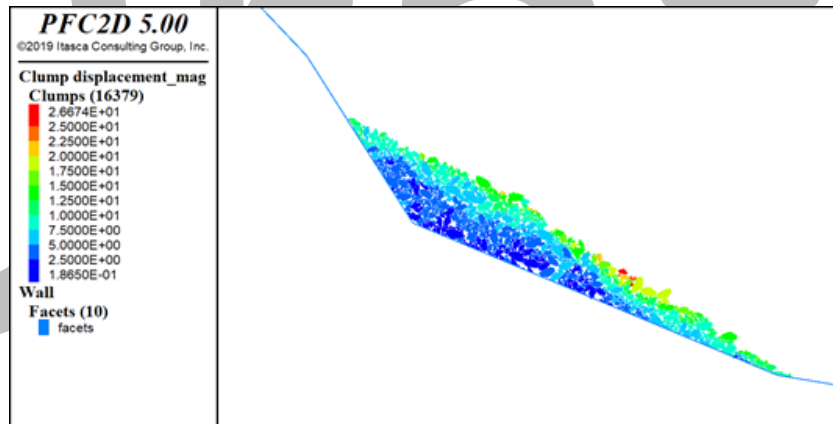


Figure 28. Displacements of the debris fan triggered by seismicity.

Field-based data retrieval

Focus

The collection of field data provides information on the geomorphological processes that are active in the mountain basin and allows to characterize the sediments from a quantitative and qualitative point of view. Moreover, it allows to estimate the potential for additional sediment supply in the basin.

Summary

The field survey for the characterisation of active processes and sediment availability focuses on two aspects. Firstly, on the quali-quantitative characterisation of sediments, which is preferably carried out at significant deposits within sedimentation basins or along the riverbed. The second aspect concerns the geomorphological characteristics of the main mountain-river courses, to estimate the removable sediments in the riverbed and to assess erosive processes along the banks. To standardise the field survey procedures, two survey forms were therefore prepared: 1) for the survey on sediment deposits; 2) for the survey along the mountain-river courses.

The procedures proposed in these guidelines were tested in five basins of the Friuli Venezia Giulia Region (Figure 29) characterised by different size, morphology, lithology, and vegetation: Rio Cucco, Rio Fella, Rio Solfo, Rio Tolina and Rio Drigniza.

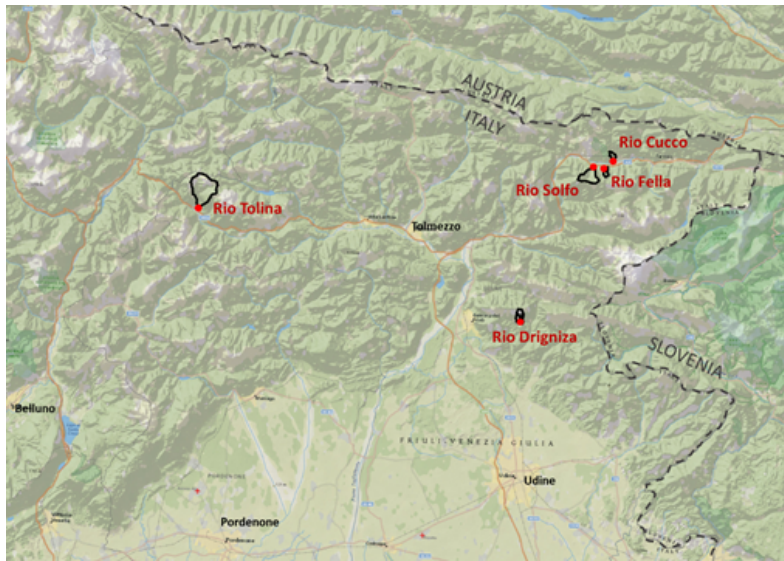


Figure 29. Location of study areas used to test and validate field survey procedures.

Measurement and recording methodologies

Description of the deposits

This survey is carried out at sediment deposits that are as representative as possible of active processes in the entire basin, preferably in downstream areas where sediments of a different nature and generated by different types of geomorphological processes accumulate. Suitable accumulations for this survey are found at the basin closure, where the lower slope contributes to the deposition of debris within hydraulic works (Figure 30a), if present, or along the riverbed (Figure 30b).



Figure 30. Suitable sites for surveying torrential deposits: a) Rio Cucco reservoir; b) Rio Drigniza riverbed.

Once a suitable deposit has been identified, the survey is carried out using the appropriate form (see Checklist section below), which is divided into four parts: 1) general assessment of the deposit; 2) assessment of the vegetative debris and dominant lithologies; 3) description of vertical profiles; 4) characterisation of the coarse debris on the surface.

1 - General assessment of the deposit. In this part of the survey, a visual estimate of the size of the deposit is made, a rough estimate of the most frequent and maximum volumes and an estimate of the ratio between coarse and fine deposit. For this purpose, it is necessary to define a size threshold between fine and coarse deposit, which is defined in the survey sheet as a diameter of 6 cm. The estimate of the ratio between coarse and fine deposit is of great importance for the subsequent reconstruction of the complete grain-size curve of the deposit because it makes it possible to estimate the volume of the upper carapace (to be characterised by UAV images, in situ photos or grid-by-number survey) and the volume of the fine deposit (to be characterised in the laboratory)

2 - assessment of the vegetative debris and dominant lithologies. This part of the survey focuses on two aspects of great importance for a possible reuse of the materials. Firstly, the presence and quantification of vegetative debris, which is to be carried out by means of visual and approximate estimation, distinguishing between fine (maximum size of vegetative debris < 0.3 m), intermediate (maximum size between 0.3 and 1 m) and coarse (maximum size > 1 m) plant debris (Figure 2). Vegetative debris is relevant from the perspective of material reuse because it constitutes a source of 'pollution' that significantly deteriorates the quality of the material. Next, the prevailing lithologies are estimated by hand analysis of some samples and estimation of the degree of chemical and physical weathering of the surface of the samples. For weathering, standard scales from grade I (unaltered surface, fresh rock) to grade V (completely weathered) are used. Both the lithology and the degree of chemical and physical weathering are relevant for reuse.



Figure 31. Examples of deposits with different proportions of plant detritus: a) metric-sized plant detritus with an aerial occupation percentage of less than 1% (Rio Drigniza); b) plant detritus between 0.3 and 1 m in size with coverage > 20% (Rio Tolina).

Term	Symbol	Description	Grade
Fresh	F	No visible sign of rock material weathering; perhaps slight discolouration on major discontinuity surfaces.	I
Slightly weathered	SW	Discolouration indicates weathering of rock material and discontinuity may be somewhat weaker externally than in its fresh condition.	II
Moderately weathered	MW	Less than half of the rock material is decomposed and/or disintegrated to a soil. Fresh or discoloured rock is present either as a continuous framework or as a corestones.	III
Highly weathered	HW	More than half of the rock material is decomposed and/or disintegrated to a soil. Fresh or discoloured rock is present either as a discontinuous framework or as a corestones.	IV
Completely weathered	CW	All rock material is decomposed and/or disintegrated to a soil. The original mass structure is still largely intact.	V

Figure 32. Weathering grades of rock mass (ISRM, 1981).

3 - description of vertical profiles. This part of the survey focuses on vertical profiles that must be excavated manually in the deposit. The thickness of the excavation depends on logistical aspects and the degree of heterogeneity of the deposit. In the presence of a deposit showing a homogeneous appearance below the carapace, it is possible to limit the thickness of the excavation to a few decimetres. Where, on the other hand, horizons with different characteristics are

recognised, it is necessary to proceed deeper to obtain a meaningful description of the deposit. Once the excavation has been made, a photographic documentation and a summary description of the deposit's characteristics are carried out. It is very important to define the thickness of the carapace, i.e., the coarsest layer whose grain size can be characterised from the surface; in this way, it will be possible to calculate the volume fraction associated with the surface grain size. At least one detritus sample should be collected for each split for laboratory analysis; in the case of heterogeneous deposits, a sample should be collected for each different facies of the deposit.

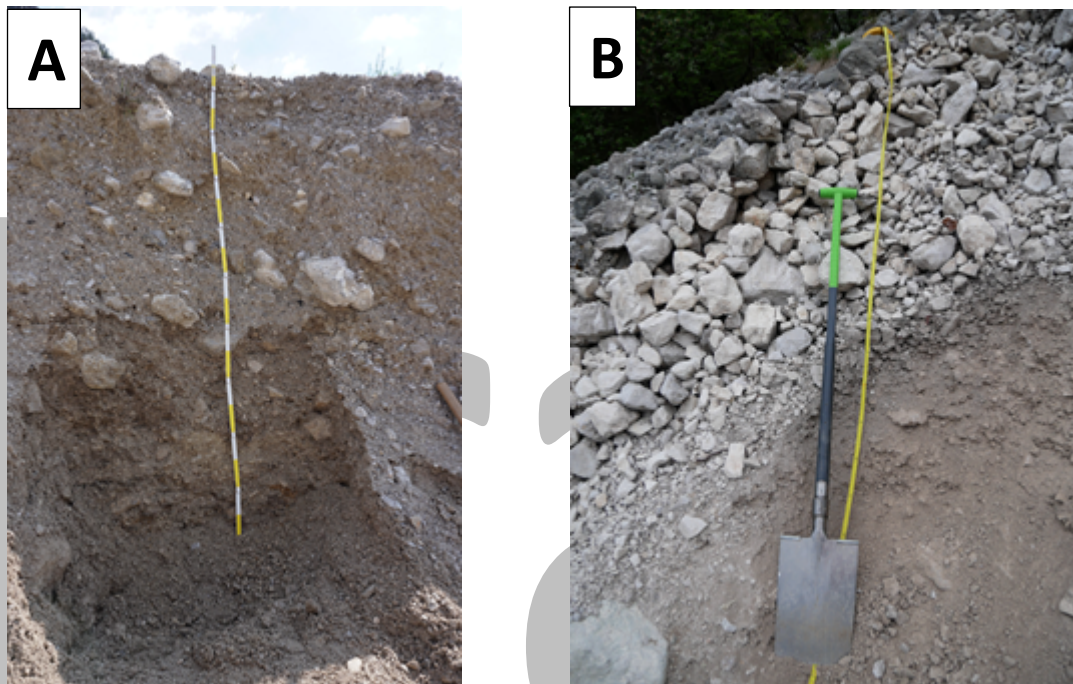


Figure 33. Examples of vertical profiles of deposits: a) profile with variations in depth over 1 m (Rio Cucco); b) homogeneous profile (Rio Drigniza).

4 - characterisation of coarse debris. The coarse surface debris can be analysed in several ways: by remote UAV survey, by photographic analysis (see next chapter) or by a grid-by-number technique. The survey sheet proposed in this project includes a simplified grid by number survey to be carried out on at least two 10 m long transects in which the grains are sampled every metre. For each sampled grain, the main axes need to be measured, while the sphericity (Figure 34) the degree of rounding, the lithology and the degree of weathering need to be estimated by eye.

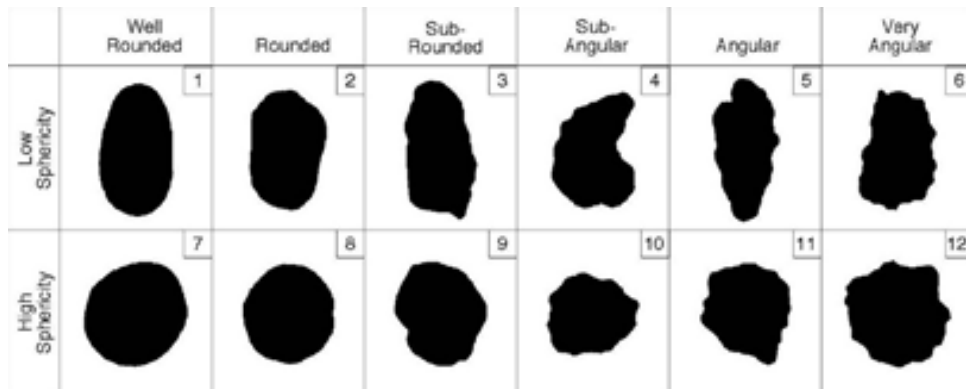


Figure 34. Sphericity guide (modified from Powers 1953 and MacLeod 2002).

Survey of mountain rivers

The purpose of this survey is to describe the geomorphologic characteristics of the main mountain rivers within the basin. The survey is carried out by walking along the riverbed and by subdividing it into reaches that are homogeneous from a geomorphological point of view. A survey form, which is attached to the checklist chapter, is then filled in for each section.

In particular, the survey is divided into seven parts: 1) delimitation of the homogeneous reach; 2) description of the riverbed; 3) description of the lithology; 4) description of the banks; 5) description of the vegetation; 6) description of the lateral sediment supply, 7) presence of obstacles and hydraulic works.

1 - Delimitation of the homogeneous reach. The identification and mapping of the homogeneous reaches (Figure xx) is carried out in the field by means of expert judgment, considering certain criteria, such as the morphology of the riverbed and slopes, the characteristics of the banks, and the presence of geomorphological processes responsible for a possible input of sediment. Homogeneous reaches typically range in size from a few tens of metres up to about 100 m in uniform rivers.



Figure 35. Example of mountain river subdivided in homogeneous reaches. In this case, the first subdivision is due to the presence of a hydraulic work, while the second is due to changes in the river flank morphology.

2 - Description of the riverbed. The riverbed in the homogeneous reach must be characterised in terms of shape (Figure 36) type of material (rock, detrital, channelled), width of the debris fill and thickness of the fill. The estimation of these last two characteristics is fundamental to make a field assessment of the sediment available in the riverbed, which can potentially be remobilized.



Figure 36. Examples of riverbeds surveyed in the test basins: a) V-shaped with debris; b) trapezoid-shaped with debris; c) channelled trapezoid-shaped.

3 - Description of the lithology and block size. The description of the lithology is carried out through estimates on hand samples. In particular, the prevailing lithology and any subordinate lithologies are reported in the sheet. As regards the size of the blocks, the sheet requires the estimation of the intermediate side of the modal size blocks, considering only the coarse fraction, i.e., those with an intermediate axis > 6 cm. The size of the largest block is made by excluding any outliers in the distribution that would be unrepresentative of the deposit.



Figure 37. Example of debris deposit in a riverbed, predominantly limestone in nature. The modal size of the coarse fraction (> 6cm mid-axis) is highlighted in red, while the block in blue is identified as the larger block, except for outliers.

4 - Description of the banks. It is requested to describe the typology of both the right bank and the left bank. The categories are slope deposit, in erosion, in rock and channelled. A possible measurement or estimate of the bank height can be added in the notes.



Figure 38. Examples of banks described during the survey: a) left bank in rock, right bank in slope deposit (Rio Cucco); b) bank in erosion (Rio Drigniza).

5 - Description of the vegetation. Both the presence of vegetative debris in the riverbed and the presence of live vegetation within the riverbed and along the banks should be observed. For vegetative debris, the survey form requires an estimation of the percentage in volume and of the modal length of the vegetative debris (< 0.3 m, 0.3 – 1 m, > 1 m).

6 - Description of the lateral sediment supply. The presence of bank processes responsible for potential debris supply is of great importance for characterising sediment availability. For each source present in each homogeneous reach, it is required to describe the type of source, the degree of connectivity (connected, not connected, partially connected) and the volume of sediments. Regarding the types, 10 categories were identified: shallow landslides, deep-seated landslides, accelerated erosion, overbanking, debris flow, debris talus, tributaries with debris, tributaries without debris, rockfalls, and debris accumulation.

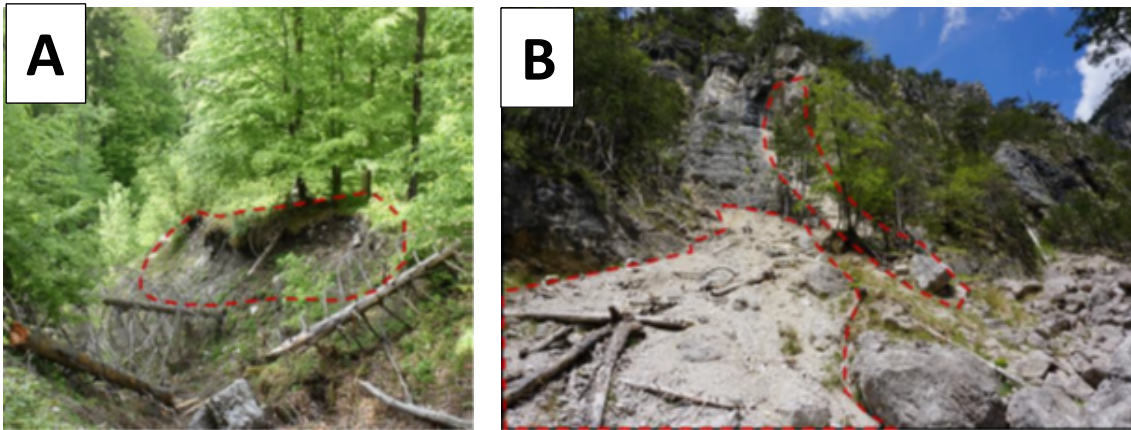


Figure 39. Examples of lateral sediment supply: a) accelerated erosion on the right bank; b) in the lower left an accumulation of debris connected to the riverbed can be seen, in the upper right a collapse landslide partially connected to the riverbed can be reckoned.

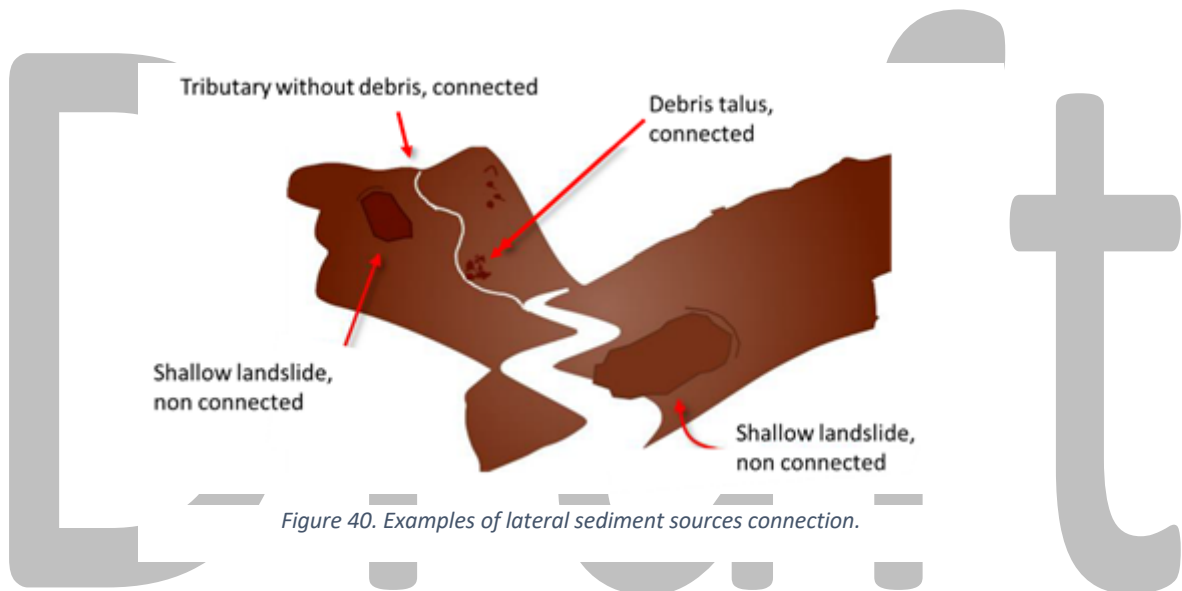


Figure 40. Examples of lateral sediment sources connection.

7 - presence of obstacles and hydraulic works. For the sediment to be effectively available for transport, it is useful to report the presence of obstacles along the riverbed or hydraulic works. The survey sheet therefore requires the identification of all obstacles present, indicating the type (moraine, alluvial fan, river terrace, crossings, and vegetation). For the hydraulic works, on the other hand, it is necessary to indicate the type (weir, check dam, repellent/panel, embankment, levee, gabion, bridge, etc.) associated with the degree of functioning (Functional, Functional damage, Structural damage, Non-functional).



Figure 41. Examples of a check dam associated with a sedimentation basin upstream (Rio Cucco).

Final products

The final products of the field data collection and analysis consist of the completed survey forms, from which it is possible to extract information on the qualitative-quantitative characteristics of the deposits and the geomorphological feature of the river reaches.

Regarding deposits, a software was developed that can reconstruct the entire grain-size curve from the field and laboratory information.

Construction of the complete grain-size curve of the deposit

To qualitatively estimate the particle size distribution of the grain constituting the deposit, the single laboratory analysis is not sufficient. This is useful for the quantification of the finer material, but insufficient for the evaluation of the coarser volumes. In contrast, an image analysis from UAV will only allow the estimation of the coarser deposits on the surface. Therefore, it is important to perform an analysis capable of unifying and harmonising particle size analyses at different scales, which allows a qualitative assessment of the entire deposit by looking at both larger and smaller grains.

According to the method proposed here, to obtain a particle size curve characterising the entire deposit, it is necessary to use:

- ✓ data from direct observation on the ground and along a vertical profile.
- ✓ data from particle size analysis performed on a sample collected on the ground from the vertical profile.

The ground observations will allow the estimation of the fine to coarse ratio of the entire deposit. Photo analysis will allow the percentage of coarse debris in the deposit to be estimated both at the surface, thanks to the UAV analysis, and at depth, thanks to the analysis of the photo from the vertical profile. On the other hand, the granulometric analysis in the laboratory will allow the fine to be quantified.

The application will use this data to estimate the particle size distribution of the deposit and provide indicative information on the possible reuse of the material.

The input files are (Figure 42):

1. Csv file of the carapace block size distribution (from UAV or photos). This shows the major and minor axes of the individual blocks mapped. It is assumed that the blocks have an ellipsoidal shape with the two minor axes equal. The file must have 3 columns: the first corresponds to the ID, the second to the major axis of the blocks (in metres) and the third the minor axis of the blocks (in metres).
2. Csv file of the vertical profile photo. This shows the major and minor axes of the individual mapped blocks. It is assumed that the blocks have an ellipsoidal shape with the two minor axes equal. The file must have 3 columns: the first corresponds to the ID, the second to the major axis of the blocks (in metres) and the third the minor axis of the blocks (in metres).
3. Csv file of the particle size analysis in the laboratory. This sheet represents the results of the sieve analysis. The sheet must have two columns: the diameter of the sieves (in centimetres) in the first column and the net weight of the passer-by at each sieve (in grams) in the second column.
4. Csv file of the laser particle size analysis in the laboratory. This sheet represents the results of the laser particle size analysis. The sheet must have two columns: the diameter of the sieves (in centimetres) in the first column and the percentage of the passer-by at each sieve (%). This file is not mandatory and can be omitted.

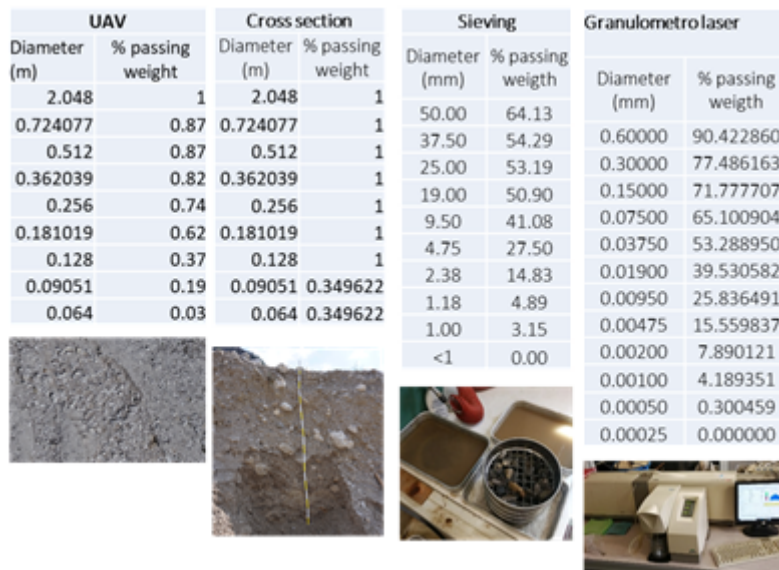


Figure 42. Example of input file for the complete grain size distribution analysis.

To combine this information, the first step is to calculate the passer-by, in terms of weight, at the sieves for each file. While this step is straightforward for the sieving and laser grain size analysis files, it is more laborious for the data from the analysis of the two images, as it requires reworking. From the orthophoto analyses, the volumes of the individual blocks were first calculated, assuming an ellipsoidal shape with the two minor axes of equal size. From this, the weight was then derived considering an average density. To obtain information on the passers-by, a digital grain size analysis was performed, i.e., grouping the mapped blocks according to the size of the minor axis, simulating what would happen in a laboratory analysis with sieves: grain size thresholds were defined corresponding to the mesh of the sieves, and it was evaluated which block passed and which did not pass for each sieve. Once the blocks were grouped according to size, the weight of the individual classes and the total weight were calculated so that the percentage passers-by from each sieve could be defined.

The passers-by derived from the input files are then combined according to the input parameters.

The input parameters required are:

- 1- Carapace thickness (Hc): Thickness of the coarse layer above the deposit
- 2- Deposit thickness (Hd): Thickness of the deposit
- 3- Percentage fines in cutaway (Ps): estimated percentage of fine material compared to coarse in the cutaway (fine coarse threshold is 6 centimetres)

- 4- Percentage fines in carapace (Pc): Percentage estimate of fine to coarse material in carapace (fine coarse threshold is 6 centimetres)
- 5- Density (ρ): density of prevailing lithology
- 6- Density of the fine (ρ_f): density of the deposit (a good rule of thumb is about 2/3 of the density of the prevailing lithology)
- 7- Fine coarse thresholds (Sf-g): threshold to identify the limit at which coarse deposits can be mapped from orthophotos and the blocks used to make the grain size.

Input parameters are required for the construction of the total grain size curve. These allow the data from the different survey scales to be harmonised to reconstruct the particle size distribution of the entire deposit.

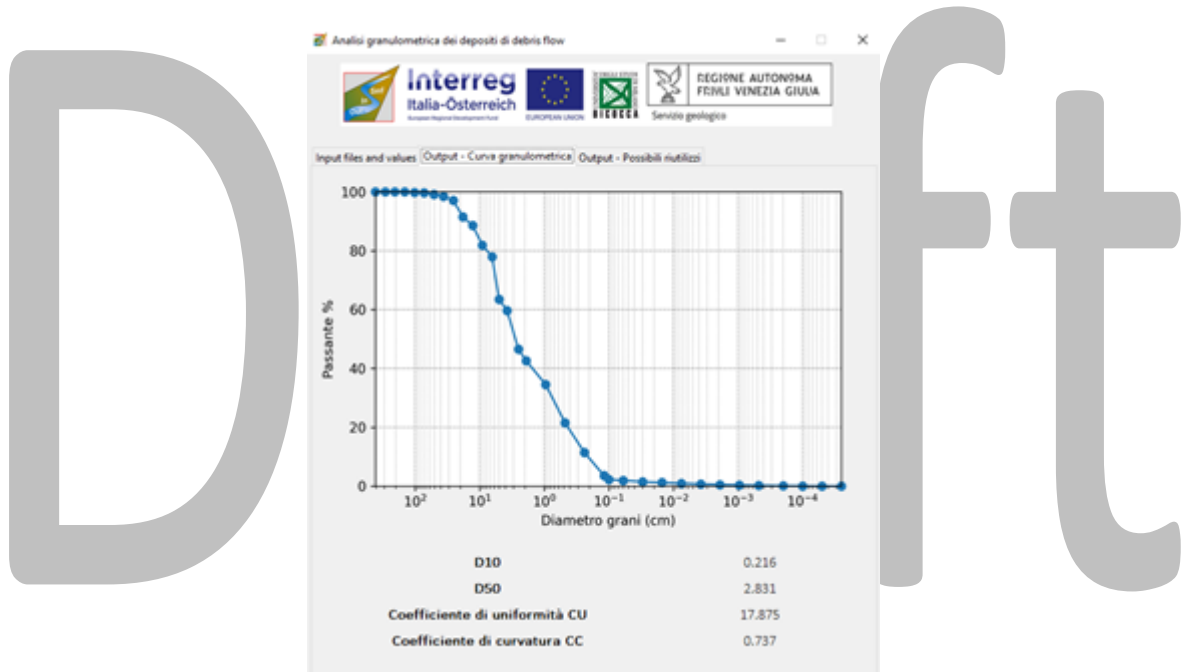


Figure 43. Output file of the software: the complete grain-size distribution.

Checklist

In this chapter the field forms are presented.

Field form for the characterization of deposits

ID:	Data:	Località:	Opera:	ID tratto:	SPZ:
-----	-------	-----------	--------	------------	------

deposito complessivo		sondrio drone	
larghezza deposito [m]:		Y	N
lunghezza deposito [m]:		campione spaccato	Y
spessore deposito [m]:		campioni blocchi	Y

volumi dei blocchi		litologia dei materiali presenti				
volumi modale [m3]		litologia	fragili	alterazione		
volumi 95th perc [m3]		chimica	W1	W2	W3	W4
volumi massimo [m3]		fisica	W1	W2	W3	W4
		chimica	W1	W2	W3	W4
		fisica	W1	W2	W3	W4
		chimica	W1	W2	W3	W4
		fisica	W1	W2	W3	W4
		chimica	W1	W2	W3	W4
		fisica	W1	W2	W3	W4
		chimica	W1	W2	W3	W4
		fisica	W1	W2	W3	W4

stima qualitativa del rapporto depositi grossolani/fine	
% fine	
% gross.	

stima del materiale vegetale presente			
	< 0.5 m	< 5 m	> 5 m
+ 3%			
+ 5%			
+ 20%			
+ 20%			

stima delle percentuali lungo spaccati							
ID spaccato	% fine < 6 cm	% fine sottocarapa	% fine carapace	% fine spaccato	spessore carapace	tipologia deposito	campione (Y/N)
1							ID foto
2							
3							
4							
5							

caratterizzazione del detrito grossolano [grid by number]	
larghezza deposito [m]:	
lunghezza deposito [m]:	
spessore deposito [m]:	
step di misura dei blocchi [cm]:	

descrizione blocchi grid by number										
ID	A1 [cm]	A2 [cm]	A3 [cm]	sfericità	arrotondamento	litologia	alterazione [SRM]			
1				A, B	MA, A, SA, ST, AT, BAT		W1	W2	W3	W4
2				A, B	MA, A, SA, ST, AT, BAT		W1	W2	W3	W4
3				A, B	MA, A, SA, ST, AT, BAT		W1	W2	W3	W4
4				A, B	MA, A, SA, ST, AT, BAT		W1	W2	W3	W4
5				A, B	MA, A, SA, ST, AT, BAT		W1	W2	W3	W4
6				A, B	MA, A, SA, ST, AT, BAT		W1	W2	W3	W4
7				A, B	MA, A, SA, ST, AT, BAT		W1	W2	W3	W4
8				A, B	MA, A, SA, ST, AT, BAT		W1	W2	W3	W4
9				A, B	MA, A, SA, ST, AT, BAT		W1	W2	W3	W4
10				A, B	MA, A, SA, ST, AT, BAT		W1	W2	W3	W4
11				A, B	MA, A, SA, ST, AT, BAT		W1	W2	W3	W4
12				A, B	MA, A, SA, ST, AT, BAT		W1	W2	W3	W4
13				A, B	MA, A, SA, ST, AT, BAT		W1	W2	W3	W4
14				A, B	MA, A, SA, ST, AT, BAT		W1	W2	W3	W4
15				A, B	MA, A, SA, ST, AT, BAT		W1	W2	W3	W4

larghezza deposito [m]:		spessore deposito [m]:	
lunghezza deposito [m]:		step di misura dei blocchi [cm]:	

descrizione blocchi grid by number										
ID	A1 [cm]	A2 [cm]	A3 [cm]	sfericità	arrotondamento	litologia	alterazione [SRM]			
1				A, B	MA, A, SA, ST, AT, BAT		W1	W2	W3	W4
2				A, B	MA, A, SA, ST, AT, BAT		W1	W2	W3	W4
3				A, B	MA, A, SA, ST, AT, BAT		W1	W2	W3	W4
4				A, B	MA, A, SA, ST, AT, BAT		W1	W2	W3	W4
5				A, B	MA, A, SA, ST, AT, BAT		W1	W2	W3	W4
6				A, B	MA, A, SA, ST, AT, BAT		W1	W2	W3	W4
7				A, B	MA, A, SA, ST, AT, BAT		W1	W2	W3	W4
8				A, B	MA, A, SA, ST, AT, BAT		W1	W2	W3	W4
9				A, B	MA, A, SA, ST, AT, BAT		W1	W2	W3	W4
10				A, B	MA, A, SA, ST, AT, BAT		W1	W2	W3	W4
11				A, B	MA, A, SA, ST, AT, BAT		W1	W2	W3	W4
12				A, B	MA, A, SA, ST, AT, BAT		W1	W2	W3	W4
13				A, B	MA, A, SA, ST, AT, BAT		W1	W2	W3	W4
14				A, B	MA, A, SA, ST, AT, BAT		W1	W2	W3	W4
15				A, B	MA, A, SA, ST, AT, BAT		W1	W2	W3	W4


Sfericità e arrotondamento		alterazione	
	W1	inalterata	
	W2	debolmente alterata / poco alterata	
	W3	moderatamente alterata <50% decomp.	
	W4	fortemente alterata >50% decomp.	
	W5	completamente alterata	

Figure 44. Field form for the characterisation of deposits.

Field form for the characterization of mountain-river course

BACINO IDROGRAFICO:		ID BACINO:	NOME CANALE:		ID ASTA:	DATA:											
sub-ID	Quota (m) /GPS	Quota (m) /GPS	ALVEO			LITOLOGIA		SPONDE		VEGETAZIONE		APPORTO SEDIMENTO LATERALE					
			Tipo (1)	Ripresa (2)	Inghessa (m) /pendimento (m)	spessore (m) /rampimento (m)	Litologie prevalente	Litologie subordinata	Ø modale (m)	Ø 95th (m)	Sponda di (3)	Sponda di (4)	detrito (5)	percento detrito (6)	INERZIA (7)	Type (8)	Connetività (9)
1																	
2																	
3																	
4																	
5																	
6																	
7																	
8																	
9																	
10																	
11																	
12																	
13																	
14																	
15																	

1	1. In roccia 2. In detrito 3. Tombinato 4. Canalizzato
2	1. trapezoidale V R. rettangolare
3	1. deposito di versante 2. in argilla 3. Rocca 4. Artificiali
4	0: No 1: < 0.5m 2: < 1m 3: > 1m
5	4: Alberi in alveo 5: Alberi su sponde 6: Arbusti in alveo 7: Arbusti su sponde
6	1. Frena superficiale (sivista) 2. Frena profonda (sivista) 3. Erosione accretata 4. Scorrimento 5. Detrita flow 6. Tappa di crollo 7. Torrente con detrito 8. Torrente senza detrito 9. crolli lungo il tratto 10. accumulo di detriti
7	1. Connesso 2. Disconnesso 3. Parzialmente discon.

sub-ID	ostacolo vite (6)	OPERA 1		OPERA 2		OPERA 3		OPERA 4		OPERA 5		ID scheda detrito	NOTE
		Tipo (10)	Stato (11) (a)	Tipo (10)	Stato (11) (a)	Tipo (10)	Stato (11) (a)	Tipo (10)	Stato (11) (a)	Tipo (10)	Stato (11) (a)		
1													
2													
3													
4													
5													
6													
7													
8													
9													
10													
11													
12													
13													
14													

8	1. Morone 2. Fari 3. Conoidi 4. Terrazzi naturali 5. Briglie continue 6. Vasche di sedimento 7. Anticamere 8. Vegetazione
10	10. Briglia 10.1. Soglia 10.2. Trabucco 10.3. Soglia a pinnacolo 10.4. Soglia 10.5. Diga spondale in cls 10.6. Scogliera in malta ric. 10.7. Sottorivista 10.8. Sottorivista in ferro 10.9. Vasca di espansione 10.10. Tombatura 10.11. Porta
11	11. Funzionante 11.1. Tratto funzionante 11.2. Tratto non funzionante 11.3. Non funzionante

Figure 45. Field form for the characterization of mountain-river course.

Sediment Analysis

Focus

The quantification and characterization of the available sediment comprises a series of action steps that all together lead to a holistic delineation of the pilot catchments sediment distribution. Sediment analysis is derived from the integration of quantitative and qualitative methods (Figure 46).

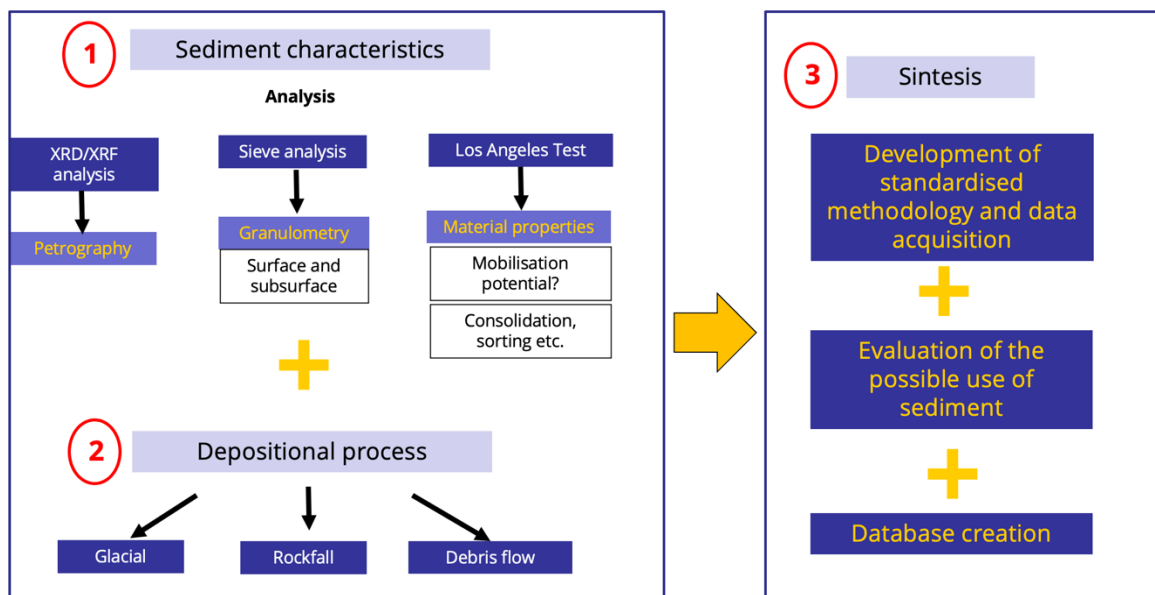


Figure 46. Workflow sediment analysis.

Summary

Sediment analysis is most accurately conducted by the delineation of both surface and subsurface grain size distributions (GSDs) along characteristic source-sink pathways within the respective pilot catchments. Therein, sediment characterization comprises the study areas *petrography* (e.g., micaschist, paragneiss, limestone etc.), *mode of sediment transport* (e.g., glacial, fluvial, mass movements etc.) as well as *bed stability* (armoring ratio).

Overall, the results emphasize the value of a quantitative sediment analysis relying on field-based sediment sample retrieval. Lab-based granulometric analysis is suitable to validate the software-

based analysis. However, it is not recommended to completely rely on software-based data. All the applications in charge are highly dependent on the quality of the input image, potentially resulting in both overestimation (coarse-grained categories) and underestimation (fine-grained categories) of grain size classes. This bias is attributable to the relationship of the clasts a- (long), b- (intermediate) and c- (short) axes. The software-based approach is limited to a 2D vision. Results obtained with GRAIN ID show a higher degree of detail and reliability compared to the results obtained with other applications (manual approach, ImageJ, JMicroVision).

Measurement and recording methodology

Field-based analysis

Field-based data analysis includes the characterization of surface (i.e., manual pebble count and photo sieving) and subsurface (i.e., bulk sampling and laboratory sieving) grain size distribution (GSD) conducted at strategic locations along the catchment's drainage network (Figure 47).

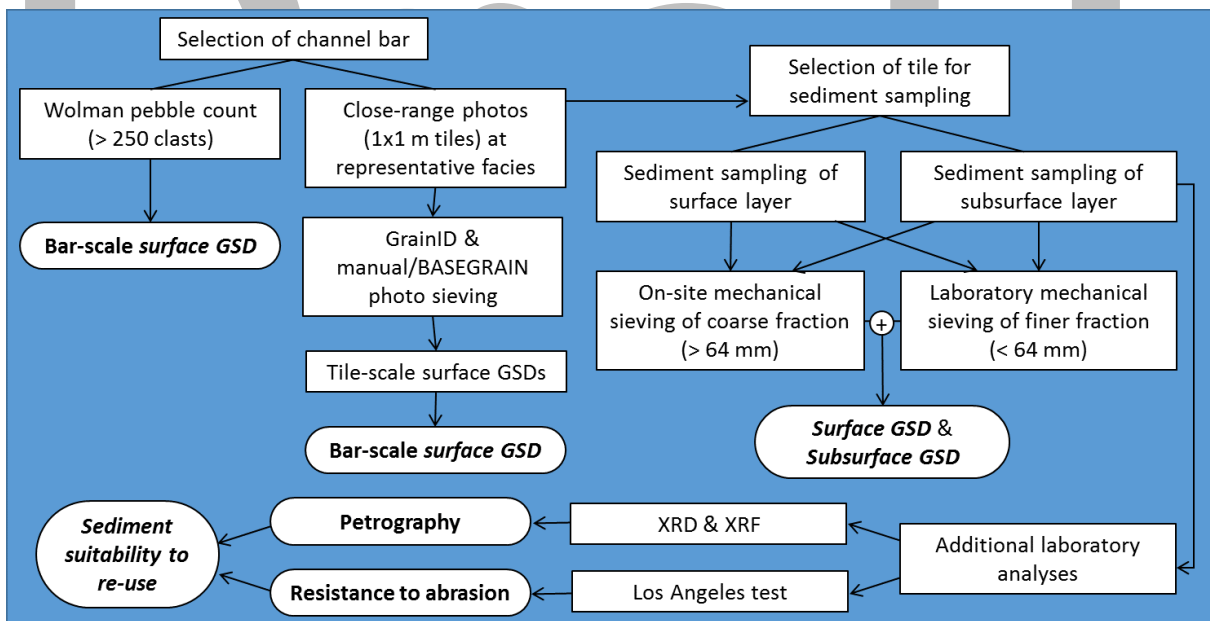


Figure 47. Methodological workflow adopted for the characterization of surface and subsurface grain-size distribution (GSD) at the sampling sites.

GSD data allows the definition of the spatial variability of characteristic sediment calibers (i.e., D50, D84, and D90) as well as the delineation of the armoring ratio (an index of channel stability), starting at glacier fronts and moving downstream (Table 10).

Table 10. Parameter of sediment analysis.

Parameter	Definition	Interpretation
D₅₀	Size point below which 50% of the material is contained	Reflecting mode of sediment transport
D₉₀	Size point below which 90% of the material is contained	Reflecting resistance structure
Armoring ratio	Ratio surface d ₅₀ and subsurface d ₅₀	Reflecting overall bed stability

Surface GSD

Method 1: Pebble-count: 50 m grid (*Wolman random walk*)

The total number of 250 randomly selected clasts is taken from a homogeneous depositional space (*grid by number approach*). The mean axis of the clasts (b-axis) is measured. Therein, the so-called "true surface grain size distribution" is determined (Table 11).

Table 11. Pebble count guidelines.

Step	Recommendation
1. Select a reach for the quantification of sediment particle size distribution	The reach should be representative of the study area.
2. Start walking at a randomly selected point	The starting position should lie at the edge of the stream.
3. Pick up the first pebble	Take one step into the water perpendicular to the flow direction and pick up the first pebble touching your index finger
4. Measure the b-axis of the clast	Put single clasts through the categories of a gravelometer, note the passing category of the clast.
5. Repeat steps 3&4	Repeat steps 3&4 until you reach the opposite side of the stream.

<p>6. Establish a new transect and repeat the process again</p>	<p>If the stream is relatively narrow you can modify the method by walking upstream in a zig-zag pattern instead of walking perpendicular to the flow direction.</p>
<p>7. Plot data in graph</p>	<p>Data plotting by size class (\log_2 scale) and frequency to determine grain size distribution.</p>

Method 2: Photo-sieving (input for software-based analysis)

To retrieve the so-called biased surface grain size distribution a comparison with close range photographs is conducted. These photographs need to be taken on a surface of 1m*1m in the same depositional space as the pebble counts that have been previously effected (Figure 48). Due to the different shape (as well as imbrication, emplacement, and coverage) of the clasts, it is probable that the true grain size and grain shapes are masked in the photos and thus incorrectly estimated.

Table 12. Workflow photo sieving.

Step	Recommendation
<p>1. Identify transect</p>	<p>The transect that is examined needs to be representative of the study area.</p>
<p>2. Take photos of single grid-sections</p>	<p>The photos need to be taken orthogonally, avoid overshadowing.</p>
<p>3. Measure long and intermediate clast axis of two clasts per grid section</p>	<p>Choose two dissimilar clasts for guaranteeing a better variance of data.</p>



Figure 48. 3-step methodology.

Subsurface GSD

Method 3: Sediment sample retrieval (input for lab-based analysis)

Sediment samples (total weight: 40 kg) are retrieved at the start and endpoint of each transect (Figure 49).

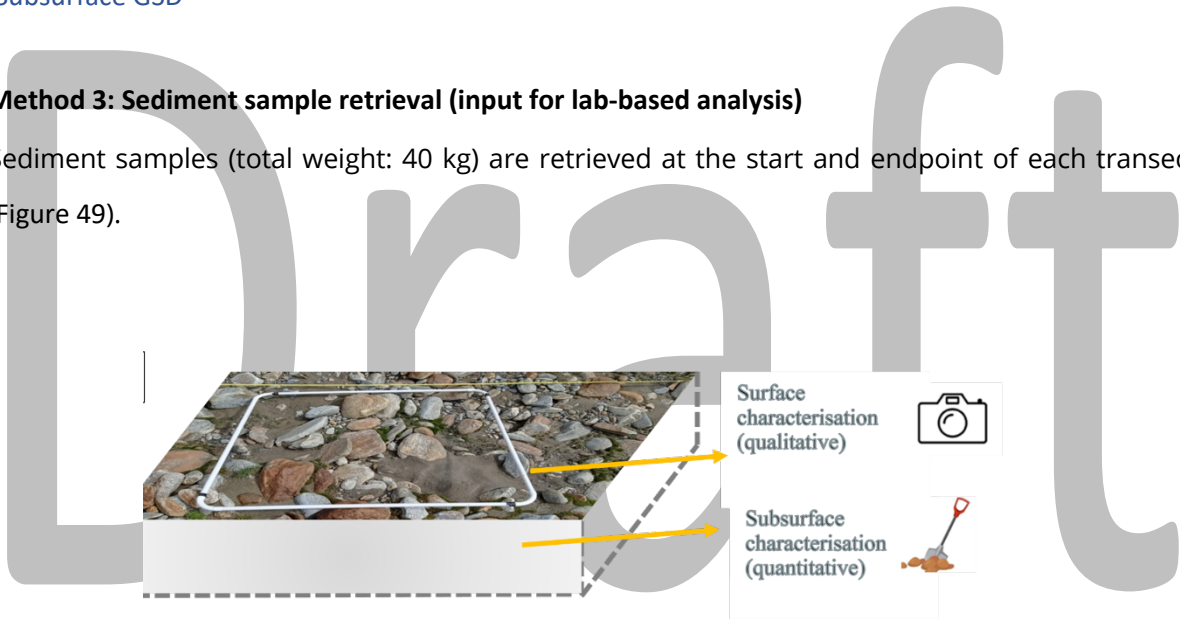


Figure 49. Top. Sediment sample retrieval procedure. Bottom. Schematic representation of sediment sampling point.

Laboratory-based analysis

Los Angeles Abrasion test

The Los Angeles Abrasion test (LAA) reflects the aggregate resistance to abrasion and fragmentation due to impact. The test measures the resistance of aggregate to wear due to attrition between rock particles and to impact and crushing by steel spheres (Ugur et al., 2010). The sample to be tested is placed together with 6-12 steel balls in a steel drum which rotates 500 times around its own axis and crushes the test material by abrasion and impact stress.

The LA-value integrates the ratio of the initial dry mass of the sample as well as the dry mass of the 1.60 mm detachment after the analysis run (Figure 50).

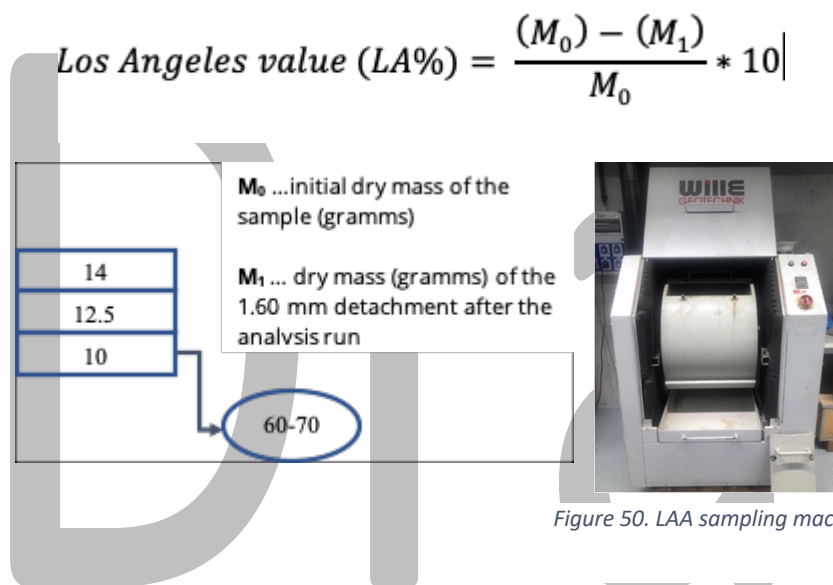


Figure 50. LAA sampling machine.

Within the aims of the SedInOut project the LG 02.12-UNI EN 1097-2 norm was implemented. The procedure consists of six working steps (Table 13).

Table 13. Action steps of the LAA test.

STEP	DESCRIPTION
1	Dry weighing of sample
2	Washing of sample
3	Additional weighing of washed sample
4	Grain fraction separation (sieve tower)
5	Sample elaboration in LA-machine
6	Calculation of LA-value

To give proper estimates about the usability of a sample the following reference values need to be considered (Table 14).

Table 14. Representative LAA-indices.

LAA-index	Usability
Up to 20	Good (for concrete, asphalt)
20-30	Medium
Over 30	Poor

XRD/XRF analysis

The X-Ray Diffraction (XRD) method counts as a powerful tool for determining the mineralogical composition of a rock sample. Therein the method consists in the calculation of the diffraction angle of the material which is beamed by X-ray transmission. During analysis three main action steps are conducted (Table 15).

Table 15. Action steps of XRD/XRF analysis.

Step	Description
1	Retrieve sediment sample (crushing of specimen)
2	Infill powder into XRD/XRF chambers
3	Analyze diffractogram with computer software (database matching profile of single minerals)

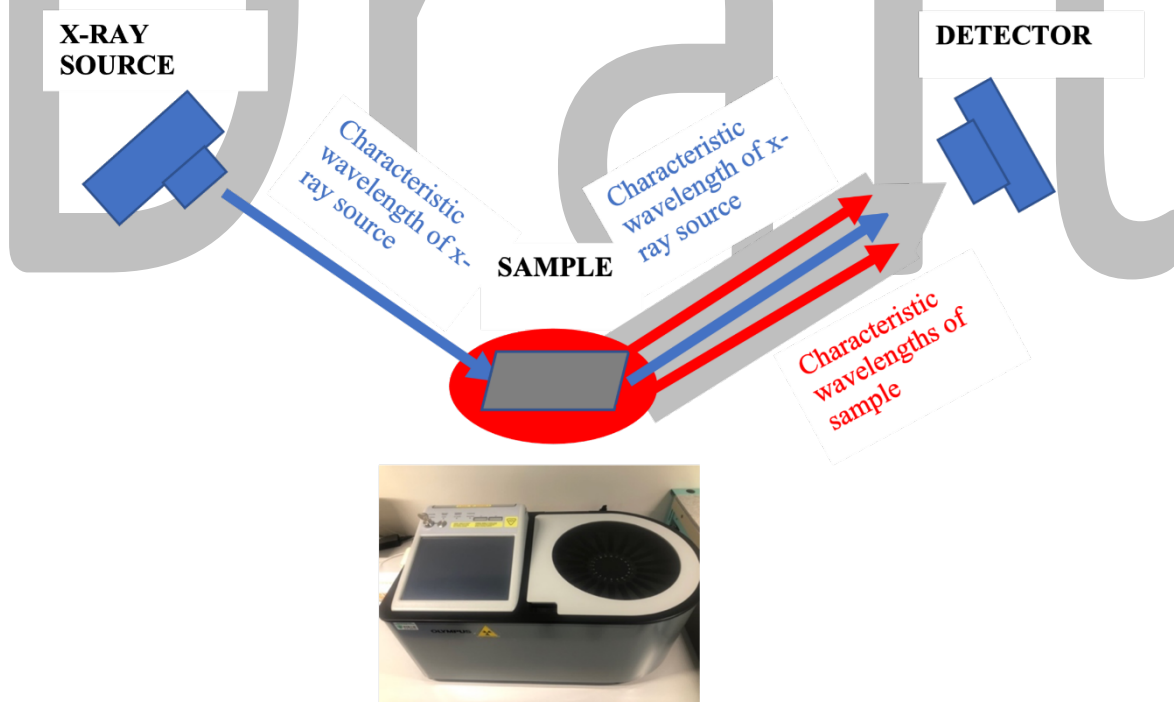


Figure 51. Schematic representation of XRD/XRF sampling.

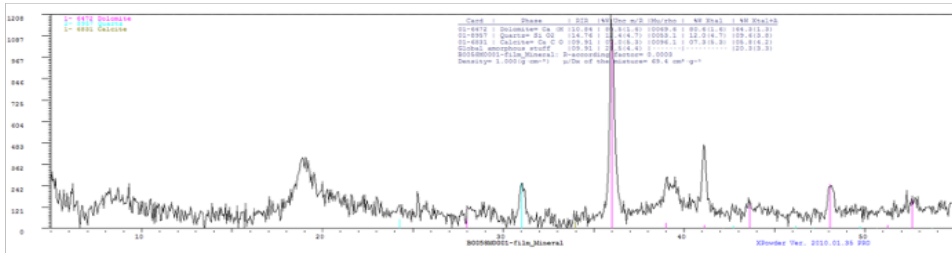


Figure 52. Sample diffractogram.

Sieve analysis

Granulometry

Preparation of sieve curves (granulometric analysis) of the sediment samples

Initially, the samples are heated overnight in the oven (105°C). According to UNI EN-933-1, 40 kg of each sample (max. grain diameter 90 mm) is weighed. Subsequently, the individual samples are washed through a coarse sieve and a fine sieve to separate the finest fractions (<0.0063 mm) from the rest of the sediment sample

The washed sample is then heated again overnight in the oven (105°C). Thereafter, the washed and dried sample is weighed to determine the percentage of fines (<0.0063 mm). Subsequently, the sample is placed in a sieve tower, separating the following grain fractions: 90 mm, 63 mm, 56 mm, 45 mm, 31 mm, 22.4 mm, 16 mm, 11.2 mm, 8 mm, 5.6 mm, 4 mm, 2 mm, 1 mm, 0.5 mm, 0.25 mm, 0.125 mm, 0.063 mm, < 0.063 mm.

Finally, the individual grain fractions are weighed, and the parameters are plotted in a sieve curve using the WinKorn software.



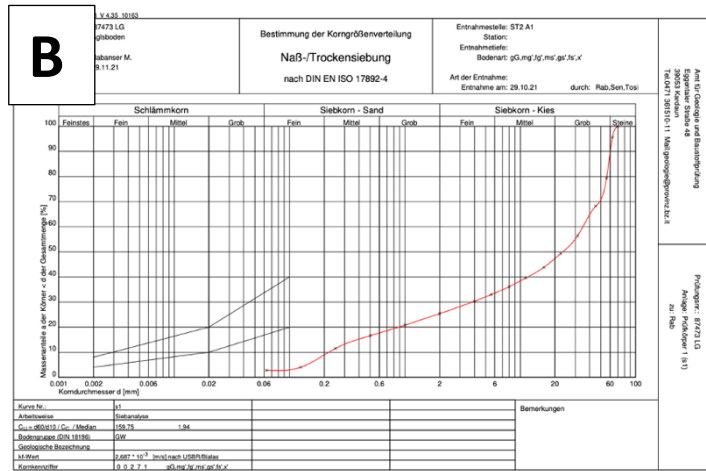


Figure 53. A. Sediment sample documentation. B. WinKorn data plot.

Software-based analysis

Main Workflow: Manual

Image retrieval & image pre-processing

The following steps are required to complete the initial phase of photo sieving (Table 16).

Table 16. Action steps required for image retrieval and image processing.

STEP	DESCRIPTION
<u>1</u>	Identify transect
<u>2</u>	Take photos of single grid sections (orthogonally, avoid overshadowing)
<u>3</u>	Draw contour lines of clasts in each photo (graphic software) to generate input images required for software-based processing

Software processing

The calibrated input images are processed with three different applications (Figure 54).

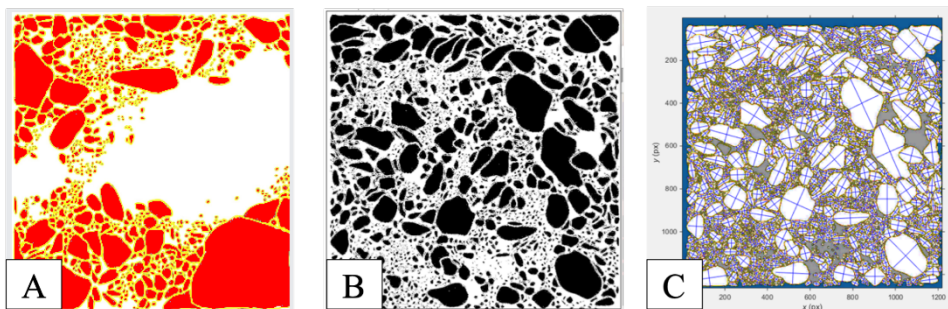


Figure 54. Examples of software-based analysis. A. J-MicroVision. B. ImageJ. C. Manual approach.

Table 17. Limitations of software-based processing.

Main limitations of software-based approach
<ul style="list-style-type: none"> • Shadow • Fine-grained material • Narrow grain interstices • Colour contrast

Main Workflow GrainID

Table 18. Description of the image processing steps composing the GrainID model framework (from Chen et al., 2022).

Step 1: Pre-processing	1.1 – image extrapolation-1	If the size (e.g., 2000×2000) of original input image could not be equally split into multiple 512×512 tiles, the image was extrapolated into 2048×2048 based on mirroring the right and down image border region.
	1.2 – image extrapolation-2	Based on the overlap-tiles strategy, for prediction of image border region, the missing context was extrapolated by mirroring the border region.
	1.3 – contrast filter	A sigmoid contrast filter in Python library Pillow was applied.
	1.4 – image augmentation	The input images were augmented by applying 0, 90 and 180° counterclockwise (CCW) rotation and horizontal and vertical flip.
	1.5 – image split	Input images were split into overlapping image tiles (512×512) as dashed red and blue rectangles in Fig. 4b.
Step 2: Prediction	2.1 – U-Net prediction	All image tiles were then sequentially input into U-Net for prediction.
	2.2 – recombination	The predicted image tiles were recombined into a full image.
	2.3 – assemble vote	The final CNN prediction was calculated as an image assembly decided by predictions from the five augmented images.
Step 3: Post-processing	3.1 – filling holes	The holes inside grains were filled.
	3.2 – filter fine grain	Unresolvable grains with size < 20 pixels were deleted.
	3.3 – narrowing interstice	An inverse watershed algorithm was applied.
	3.4 – watershed algorithm	A watershed algorithm was performed for further separation.

Table 19. Software characteristics.

<i>Application</i>	<i>Description</i>	<i>Workflow</i>	<i>Advantages</i>	<i>Disadvantages</i>
JMicroVision	Determine particle sphericity	1- <u>Spatial Calibration</u> : set image scale 2- <u>Background</u> : assign matrix 3- <u>Object Extraction</u> : identify grains	-Accurate object extraction -Multiple features can be applied	-Time-consuming -Manual effort bears the possibility for errors (clicking pixels) ☑Reliable on high-quality input image
Image J	Determine particle roundness	1-Image -> Type -> 8bit 2-Image -> Adjust -> THRESHOLD (assign pixel threshold, that correlates with the grains) 3-Process -> Analyze particles	-Time efficient -Multiple features can be applied	-Object extraction less accurate -Manual effort bears the possibility for errors (adjusting threshold) Reliable on high-quality input image Roundness parameter as median of roundness of grain
Manual approach	Determine superficial granulometry	1-Scaling 2-Object view (corrections) 3-Generate graph (surficial granulometry)	-Time efficient -User friendly interface	-Object extraction not always accurate (grain interstices falsely detected) -Manual effort bears the possibility for errors (adjusting false grain classifications) -Reliable on high-quality input image -requires extensive parameter tuning, significant level of expertise, performs poorly in fluvial environments
Grain ID	Determine superficial granulometry		- High predictive accuracy (comparable to manual labeling) - Vegetation has little influence on performance	Common limitations: -Shadow -color-contrast -narrow grain interstices -fine-grained material (resolution limit)

Examples of software-based processing

Limitations Manual approach

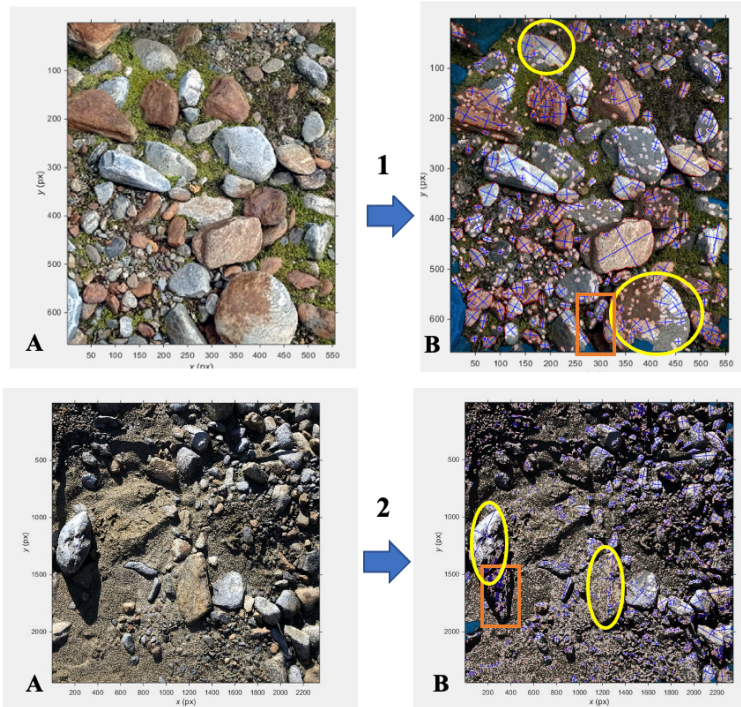
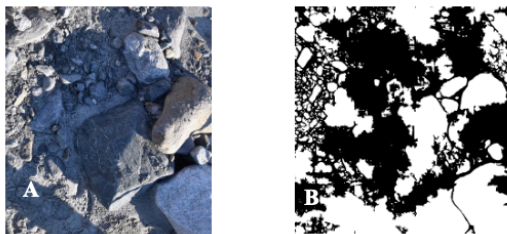


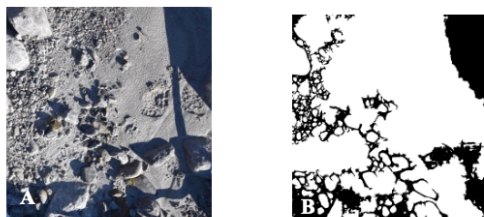
Figure 55. Practical examples operating with the manual approach. A. Original image. B. Result of image processing (operation mode: automatic detection).

Specific difficulties exist in the correct detection of larger grain size classes (yellow circles) and shadow areas (orange rectangles).

Limitations GrainID



Limitation: shadowed area
Proglacial 1 a-8



Limitation: Shadow + fine-grained material
Proglacial 1 b-13

Figure 56. Practical examples operating with GrainID.

Final products

Assessment of characteristic source-sink pathways in Val di Mazia and Val Ridanna

To classify the sediment transport both qualitatively (sediment pathways) and quantitatively (surface and subsurface grain size distribution) a series of characteristic source to sink pathways were studied in the lead partners pilot areas.

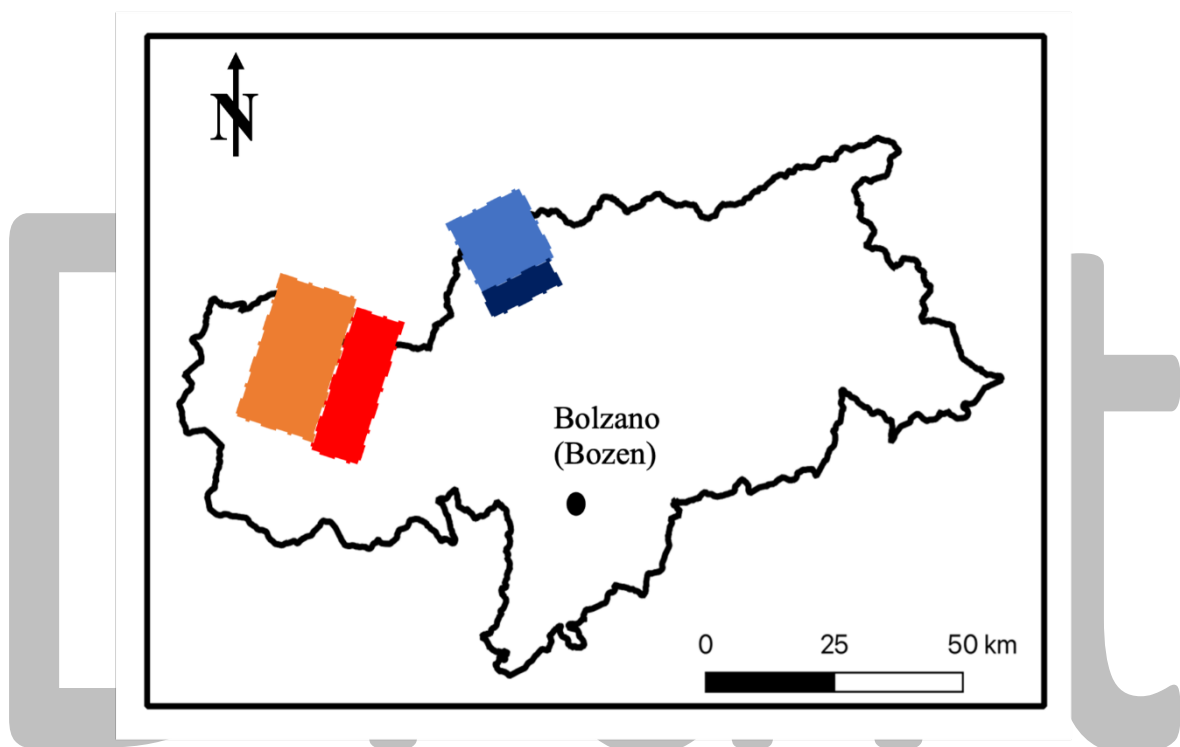


Figure 57. Pilot areas in the Autonomous Province of South Tyrol (N-Italy). Mazia (Matschertal) valley (orange rectangle), Senales (Schnalstal) valley (red rectangle), Upper Ridanna (Oberes Ridnauntal) valley (light blue rectangle), Lazzago (Lazzachertal) valley

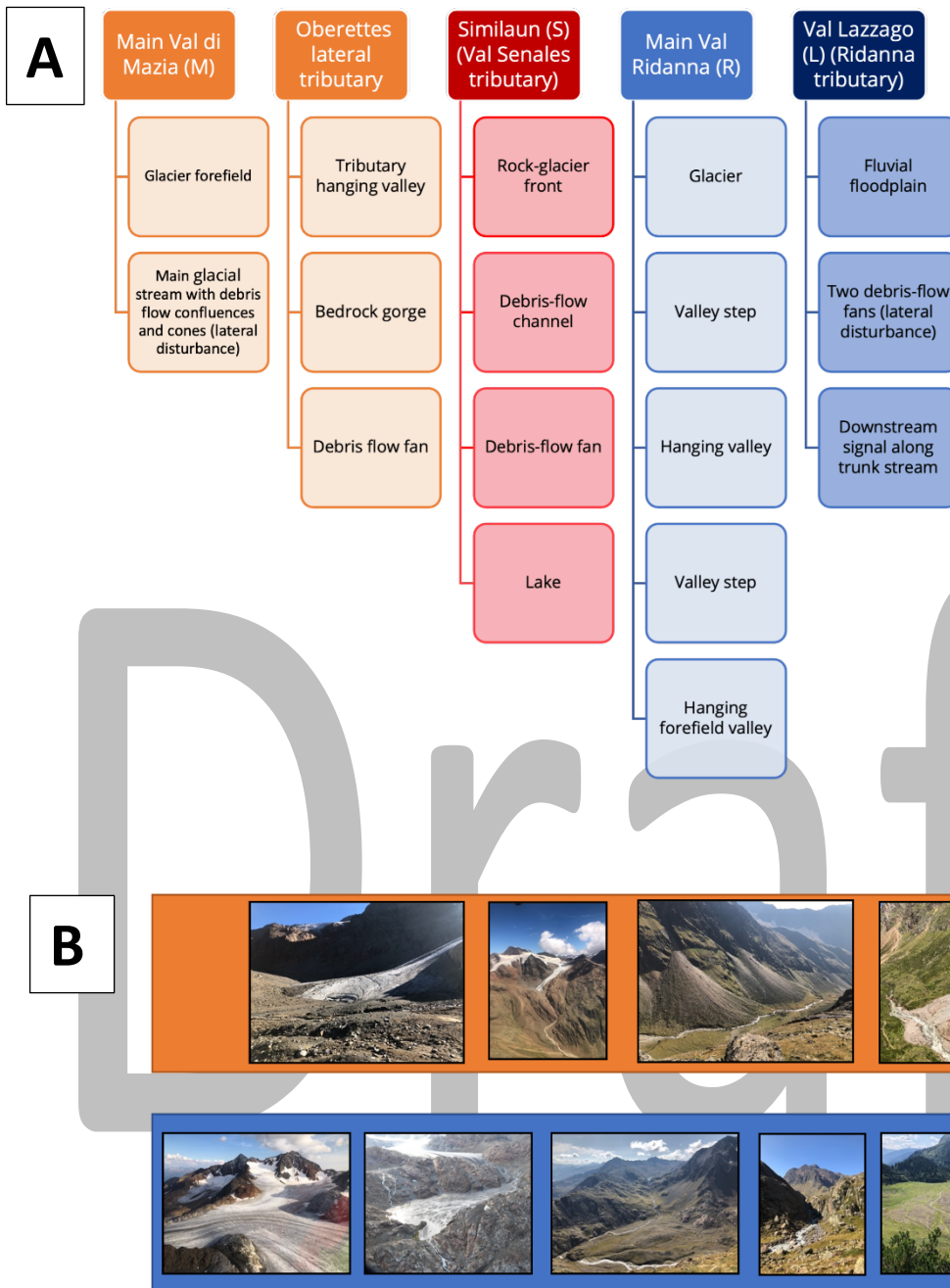
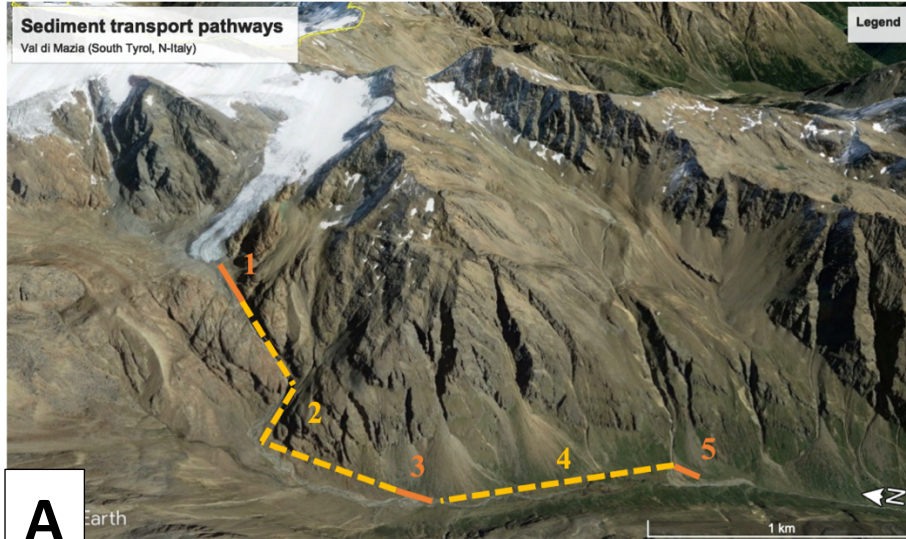
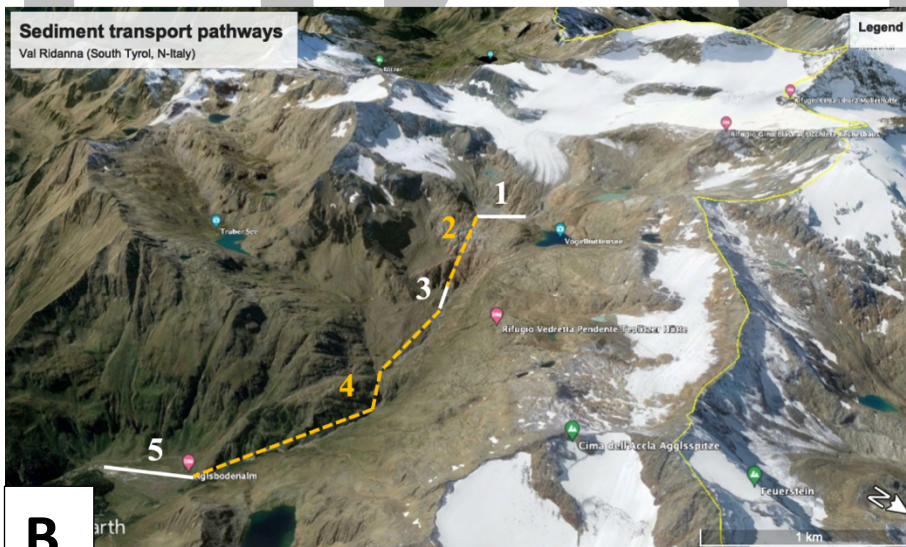


Figure 58. Source to sink pathways studied in the pilot areas of the project lead partner. A. Flowchart. B. Field impressions.

Sediment transport pathways in Mazia and Ridanna valleys



- 1...Proglacial plain
- 2...Valley step 1
- 3... Alluvial plain
- 4...Valley step 2
- 5...Debris cone



- 1...Proglacial plain
- 2...Valley step 1
- 3...Grohmann plain
- 4...Valley step 2
- 5...Aglsboden plain

Figure 59. Sediment transport pathways. A. Mazia valley. B. Ridanna valley.

Channel bed texture and armor ratio (Example: Mazia valley)

Comparison of surficial grain size distributions (GSD) obtained respectively through field-based Wolman pebble count (Wolman, 1954) and through GrainID-based processing of close-range vertical photos (Chen et al., 2022) exhibits substantial agreement, with a tendency for the latter to generate comparably coarser distributions (**Table**). We observe virtually identical D50 at sites M2 and M4, and to a limited extent, coarser GrainID-based D50 at the other sites, with an offset ranging between 5 mm (M3) and 15 mm (M5). This tendency is even more apparent for coarser fractions at all sites, where: (i) offset in D84 ranges from 14 mm to 47 mm; and (ii) offset in D90 ranges from 26 mm to 84 mm (**Table**).

As for subsurface GSD, obtained from on-site sediment sieving of material coarser than 64 mm (i.e., “Lab”) followed by laboratory sieving of the finer fractions (i.e., “Field”), we show the importance of integrating these two methodological steps for capturing the entire range of grain size variability. At all sites except M2 – the hanging braided alluvial plain characterized by particularly fine GSD that did not require on-site sieving – results show how laboratory sieving alone would yield markedly underestimated subsurface grain size percentiles. Underestimation ranges: (i) from as little as 15 mm up to a maximum of 38 mm, in terms of D50; (ii) from 27 to 86 mm in terms of D84; and (iii) from 28 to 105 mm in terms of D90. In turn, subsurface underestimation of sediment caliber propagates down to the calculation of armor ratios, which would result 3 to 4.3 times larger than field-integrated analogues.

Table 20. Sampling site attributes, and characteristic surface and subsurface grain size percentiles constrained by means of several techniques.

Site	Elevation (m a.s.l.)	Slope (m/m)	Drainage area (km ²)	Surface (mm)						Subsurface (mm)					
				Wolman			GrainID			Lab			Field & Lab		
				D ₅₀	D ₈₄	D ₉₀	D ₅₀	D ₈₄	D ₉₀	D ₅₀	D ₈₄	D ₉₀	D ₅₀	D ₈₄	D ₉₀
M1	2730	0.10	1.3	56	110	126	62	157	210	1	32	40	42	98	108
M2	2850	0.01	0.6	21	40	45	21	54	71	7	22	26	7	22	26
M3	2405	0.11	7.6	57	134	157	62	169	213	10	30	36	42	72	80
M4	2280	0.20	1.8	57	101	116	56	120	146	9	33	38	35	60	66
M5	2240	0.08	13.8	45	91	114	60	125	152	12	27	30	50	113	135
M6	2240	0.07	1.4	na	na	na	37	72	84	7	23	27	22	67	75

Table 21. Sensitivity analysis of armour ratios to variable surface and subsurface GSD data types.

Site	Armour ratio			
	Wolman/Lab	GrainID/Lab	Wolman/Field & Lab	GrainID/Field & Lab
M1	5.57	6.16	1.34	1.49
M2	3.10	3.10	3.10	3.10
M3	5.61	6.09	1.35	1.46
M4	6.12	6.01	1.64	1.62
M5	3.82	5.10	0.90	1.20
M6	na	5.01	na	1.69

Along Saldur Creek, surface D50 remains about constant from the glacier forefield (56-62 mm at M1), across the LIA moraine area (57-62 mm at M3), and down to the confluences with the two lateral tributaries (45-60 mm at M5). By contrast, D84 and D90 both exhibit limited downstream coarsening at M3, followed by drastic fining at M5 (i.e., values at M5 are smaller than at M1; Table 4.5), hence suggesting that adjacent, steep lateral tributaries do not supply coarser bed material. This observation is supported by the GSD downstream pattern in Oberettes Creek, where fine D50 in the braided hanging floodplain (21 mm at M2) coarsens at the fan terminus (56-57 mm) and attains values identical to those recorded at M5. The same spatial pattern applies to D84 and D90 (Table 4.5). Along these lines, we find that Unnamed Creek supplies to Saldur Creek substantially finer material, as indicated by D50 (37 mm), D84 (72 mm) and D90 (84 mm) recorded at the fan terminus (M6).

With reference to subsurface GSD, the spatial patterns of subsurface D50, D84 and D90 present differences and similarities with what was observed for the surface counterparts. The main difference relates to Saldur Creek main stem, where: (i) D50 remains constant between M1 and M3 (42 mm) but coarsens at M5 (50 mm); and (ii) D84 and D90 display downstream fining from M1 (98-108 mm) to M3 (72-80 mm), and substantial coarsening further downstream at M5 (113-135 mm). Similarities with surface GSD patterns relate to: (i) subsurface downstream fining between M2 and M4 along Oberettes Creek; and (ii) subsurface sediment percentiles (i.e., D50, D84 and D90) at tributary fan termini (sites M4 and M6) being substantially finer than the receiving Saldur Creek (site M5).

The combination of the foregoing surface and subsurface GSD variability generates remarkably consistent pattern of channel stability across the sampling sites, which range from gentle glacier forefields (1.3 km²) to steep reaches nested in alluvial fans (1.8 km²), and turbulent braided reaches along a main glacial trough (13.8 km²). Namely, armour ratios range between 1.49 and 1.69 when using GrainID-derived data, and between 0.90 and 1.64 when using Wolman-based ones. In this context, site M2, possibly the most purely fluvial site, stands out for being the most stable with an armour ratio of 3.10.

Sampling Mazia valley 2021

Surface (Wolman pebble count)

Surface (Grain ID): software-based approach

Subsurface (laboratory sieving <90 mm)

Subsurface (Field+Lab: field-weighing > 63 mm + laboratory sieving <90 mm)

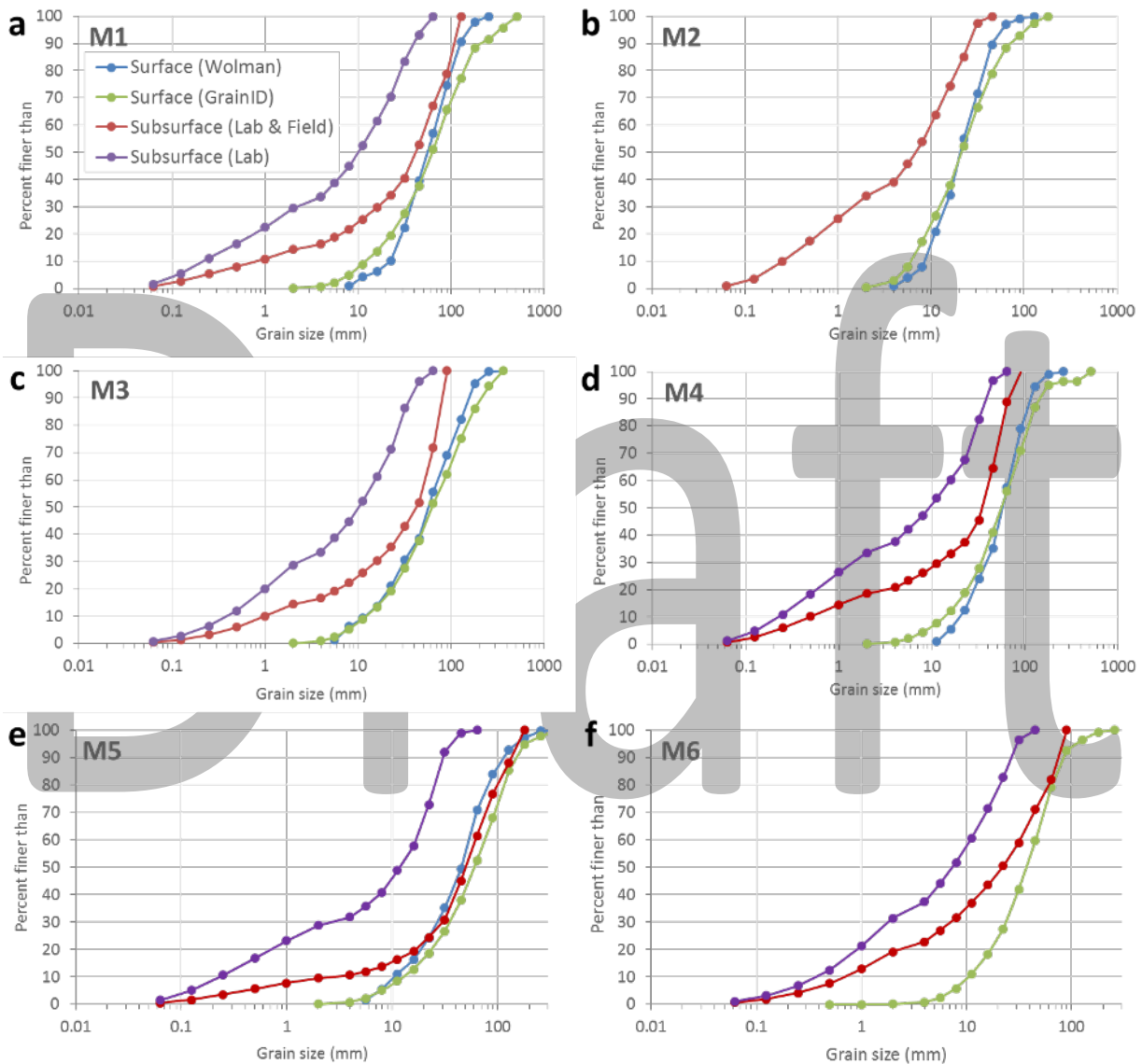


Figure 60. Surface and subsurface grain size distributions (GSD) at the six sampling sites in Upper Mazia Valley.

Sampling Mazia valley 2022

Surface (Field+Lab): field weighing > 63 mm + laboratory sieving < 90 mm

Surface (Manual): software-based approach

Subsurface (Lab): laboratory sieving < 90 mm

Subsurface (Field+Lab): field weighing > 63 mm + laboratory sieving < 90 mm

Table 22. Surface and subsurface parameters.

Site	Surface (mm)						Sub Surface (mm)					
	Manual			Field + Lab			Lab			Field+Lab		
	D ₅₀	D ₈₄	D ₉₀	D ₅₀	D ₈₄	D ₉₀	D ₅₀	D ₈₄	D ₉₀	D ₅₀	D ₈₄	D ₉₀
M-ST1-A1	72	262	286	102	144	158	12	32	41	71	212	268
M-ST1-A2	74	228	286	78	123	135	18	39	50	36	118	137
M-ST2-A1	23	138	178	64	90	105	17	42	52	22	113	133
M-ST2-A2	23	73	88	87	138	161	19	51	54	91	169	174
M-ST3-A1	22	71	91	73	121	147	12	42	43	31	90	113

Table 23. Armor ratios Mazia valley (sampling 2022).

Site	Armor ratio			
	Manual/ Lab	Field + Lab _{surface} / Lab	Manual/ Field+Lab _{subsurface}	Field+Lab _{surface} / Field+Lab _{subsurface}
M-ST1-A1	6	8.5	1.01	1.43
M-ST1-A2	4.11	4.33	2.05	2.16
M-ST2-A1	1.35	3.76	1.04	2.90
M-ST2-A2	1.21	4.57	0.25	0.95
M-ST3-A1	1.81	6.08	0.70	2.35

Decision-making process

Project-specific recommendations:

- Conduct an accurate field survey, including a detailed mapping of the system components. Define characteristic source-sink pathways and focus on the multitemporal evolution of the pilot catchment
- Conduct quantitative lab-based sediment analysis (based on field-based sediment sample retrieval). Establish grain size distribution curves of both surface and subsurface sediment samples and calculate the armoring ratio.
- Need for further software refinement.

Checklist

Fieldwork: List of materials

Table 24. List of materials.

Material	Check
Sampling bags (20-30)	
Shovel	
Spade	
Wood panels	
Clippers	
Permanent marker	
Frame (reference scale for taking photographs of surface sediment distribution)	
Tape measure	
Spray can	
Notebook	
Pen	
Camera	
Tripod (fixing camera in orthogonally to the surface)	
Gravelometer	
Field scale	

Fieldwork: Sample retrieval

Table 25. Sample retrieval.

STEP	Recommendation	Check
1- Identify transect	The transect that is examined needs to be representative of the study area	
2- Take photos of single grid sections on transect	The photos need to be taken orthogonally, avoid overshadowing	
3- Measure long and intermediate clast axis of two clasts per grid section	choose two dissimilar clasts for guaranteeing a better variance of data	
4- Retrieve sediment samples from starting and end of the grid section (40 kg per transect)	Retrieve 20 kg of sediment material at the starting and end point of the transect. Important: remove superficial layer before retrieving the sample.	
5- Quantitative description of the sediment sample	Estimate amount of organic material (roots, wood pieces) and anthropogenic impact	
6- Estimation of sediment history	Single or compound events of sediment deposition -> holistic view	

Labwork: Granulometry

Table 26. Granulometry.

STEP	Description	Check
1. Sample preparation	Extract samples from sampling bags and put them in the oven (overnight 105°C)	
2. Sample weighing, I	Weigh 40 kg of each sample	
3. Sample washing	Wash sample through stack of fine sieves to separate the fine fractions (<0.0063 mm)	
4. Sample drying	Put washed sample in the oven (overnight 105°C)	
5. Sample weighing, II	Weigh washed and dried sample to determine the number of fines (<0.0063 mm)	
6. Sieve analysis	Put sample into sieve stack (90 mm, 63 mm, 56 mm, 45 mm, 31 mm, 22.4 mm, 16 mm, 11.2 mm, 8 mm, 5.6 mm, 4 mm, 2 mm, 1 mm, 0.5 mm, 0.25 mm, 0.125 mm, 0.063 mm, < 0.063 mm)	
7. Sample weighing, III	Weigh single grain fractions	
8. Plot data into sieve curve	Type in parameters in WinKorn application to display sieve curve and to determine grain size distribution	

Sediment use

Focus

The reuse of sediment that accumulates in debris deposits is an important goal from the perspective of the circular economy. The purpose of this chapter is to describe in a very practical way the possible uses of sediment in compliance with quality criteria defined by regulations or by national and international standards.

Summary

Sediments that accumulate in mountain basins, such as within retention and sedimentation basins, are a problem for the efficiency of hydraulic works, as well as a potential source of danger when remobilized by flood events. For this reason, it is essential that sediments be removed regularly to maintain high efficiency of the works. The commonly used practice is the disposal of sediments as waste, with a related cost and loss of potential resources.

This chapter describes the possible uses of sediments and defines the limitations to use arising from national and international regulations and standards.

As seen in Table xx, eleven possible reuses of the materials have been identified, for eight of which reference standards have been collected. The limitations are of four types: particle size, physical/mechanical, petrographic, and mineralogical.

Table 27. List of major uses of stone sediments and identification of limitations to use.

	Grain-size limitation	Physical mechanical limitation	Petrographic limitation	Mineralogic limitation
Railway ballast	x	x		
Gabions	x			
Fine aggregate for concrete	x		x	
Coarse aggregate for concrete	x		x	
Aggregates for asphalts	x	x	x	
Cements			x	
Soil corrections	x		x	
Paving			x	
Embankments and in-situ cementing				

Pigments	x		x	X
Plastic fillings	x		x	x
Gardening	x			

Railway ballast

The gravel shall be subjected to the following laboratory tests:

Particle size analysis	Frost-thaw resistance
Content in fine particles	Volumetric mass of particles
Content in fine	Water absorption coefficient
Shape index and long elements	Compressive strength test
Fragmentation resistance Los Angeles	Mineralogical-petrographic microscopic analysis on thin section

Particle characteristics

Grainsize

<i>sieve opening (mm)</i>	80	63	50	40	31.5	22.4
<i>passing fraction (%)</i>	100	100	70-99	30-65	1-25	0-3

Fraction between 31.5 and 50 mm must not be less than 50 %. On a 60 kg sample (lower weight sample not valid) the 0.5 mm sieve passing fraction must not exceed 0.6% (UNI EN 9331-1). On a 60 kg sample, the 0.063 mm sieve passing fraction for wet sieving must not exceed 0.5% (UNI EN 933-1).

Particle shape

Request category SI 20 of the UNI-EN 13450 leaflet. Shape factor calculated on a sample of at least 40 kg. The percentage by weight of elements with a minimum size less than 1/3 of the maximum must not exceed 20%.

Particle length

Category B of EN 13450 required. The weight percentage of elements with a length greater than or equal to 100 mm, measured on a 40 kg sample of crushed stone, must not exceed 6%.

Mechanical/physical properties

Fragmentation resistance - Los Angeles (LA) test

$$LA_{RB} = \frac{P_i - m}{P_i} \times 100$$

Where

P_i = initial mass of the test sample expressed in grams

M = mass retained on the 1.6 mm sieve in grams

Coefficient L.A.	RFI Category	Category L.A. RB
≤16%	1	LA _{RB} 16
≤20%	2	LA _{RB} 20
≤26%	3	LA _{RB} 26

Durability - Resistance to freezing and thawing

$$\Delta S_{LA} = \frac{S_{LA1} - S_{LA0}}{S_{LA0}} \times 100$$

Where

S_{LA0} is the Los Angeles coefficient of the test sample without freeze-thaw cycles

S_{LA1} is the Los Angeles coefficient of the test sample after freeze-thaw cycles

Non-freezing crushed stone	$\Delta S_{LA} \leq 20$ PER CENT
-----------------------------------	----------------------------------

Volumetric mass of particles

The crushed stone is considered suitable if the particle volume mass is > 2.55 Mg/m³.

Water absorption coefficient

Crushed stone is considered suitable if the water absorption of the particles is ≤ 2%, for RFI categories 1 and 2, and ≤ 3% for category 3.

RFI Categories	Coeff absorption
1	≤2%
2	
3	≤3%

Lithological classification

The lithological classification of the crushed stone shall be carried out by determining the presence, in percentage, of the principal and secondary minerals and shall be expressed according to the IUGS nomenclature in scientific terminology. The lithology shall be determined based on macroscopic examination of the sample, mineralogical-petrographic analysis on thin section under a polarising microscope and, if necessary, for volcanic rocks only, by chemical analysis, using QAPF and TAS diagrams. The ballast for railway ballast shall not have a content in dangerous components or substances that exceeds the limits established by the legal and administrative regulations. It is not permitted to use ballast for railway ballast produced from rocks commonly known as "green stones", whose denomination and mineralogical content is reported in annex 4 to the Ministerial Decree of the Ministry of Health dated 14/5/1996, published in the Official Gazette no. 251 dated 25/10/1996, as well as from those rocks characterised by conditions of alteration and paragenesis, such as to present a potential risk for the presence of asbestos minerals. The crushed stone shall not contain asbestos minerals pursuant to Art. 247 of Legislative Decree no. 81 of 09/04/2008. The determination of the presence of asbestos minerals shall be carried out on the same thin sections used for the lithological classification and at the same time as this (microscopic mineralogical-petrographic analysis on thin section).

Gabions

Geometric characteristics

Sieve opening (cm)	25	15
Passing fraction (%)	100	0

The blocks must not be too regular in shape

Fine aggregate for concrete (ASTM)

Particle characteristics

sieve opening (mm)	9.5	4.75	2.36	1.18	0.6	0.3	0.15
<i>passing fraction (%)</i>	100	95-100	80-100	50-85	26-60	5-30	0-10

No more than 45% of the material passing through a sieve must be blocked at the next sieve.

Dangerous substances

The quantity of fine hazardous materials must not exceed the limits prescribed in the table:

	Maximum mass percentage for the sample
Clay and crumbly rocks	3

Coal and lignite	0.5
Other aggregates	1

Fine aggregates should be free of impure organic materials.

If the aggregate is subject to wetting, it must not contain materials that react with the alkali in the cement in sufficient quantity to cause excessive expansion of mortar or concrete. Use aggregates with a cement containing an average of 0.6% of alkali or with the addition of material that prevents expansion resulting from the alkali-aggregate reaction.

Soundness

Fine aggregates subjected to 5 soundness test cycles should have an average weight loss of no more than 10% when using sodium sulphate or 15% when using magnesium sulphate.

Coarse aggregates for concrete (ASTM)

Geometric characteristics

Sieve number	opening sieves (mm)	100	90	75	63	50	37.5	25	19	12.5	9.5	4.75	2.36	1.18	0.3
1	Passing (%) (90 to 37.5 mm)	100	90-100		25-60		0-15		0-5						
2	passing (%) (63 to 37.5 mm)			10-100	90-100	35-70	0-15		0-5						
3	Passing (%) (50 to 25.0 mm)				100	90-100	35-70	0-15		0-5					
357	Passing (%) (from 50 to 4.75 mm)				100	95-100		35-70		10-30		0-5			
4	Passing (%) (37.5 to 19.0 mm)					100	90-100	20-55	0-15		0-5				
467	passing (%) (37.5 to 4.75 mm)					100	95-100		35-70		10-30	0-5			
5	Passing (%) (25.0 to 12.5 mm)						100	90-100	20-55	0-10	0-5				
56	Passing (%) (25.0 to 9.5 mm)						100	90-100	40-85	10-40	0-15	0-5			
57	passing (%) (25.0 to 4.75 mm)						100	95-100		25-60		0-10	0-5		

6	passing (%) (19.0 to 9.5 mm)							100	90-100	20-55	0-15	0-5				
67	passing (%) (19.0 to 4.75 mm)							100	90-100		20-55	0-10	0-5			
7	passing (%) (12.5 to 4.75 mm)								100	90-100	40-70	0-15	0-5			
8	passing (%) (9.5 to 2.36 mm)									100	85-100	10-30	0-10	0-5		
89	passing (%) (9.5 to 1.18 mm)										90-100	20-55	5-30	0-10	0-5	
9	passing (%) (4.75 to 1.18 mm)										100	85-100	10-40	0-10	0-5	

Dangerous substances

classes	Type or use of concrete	Maximum allowance %						
		Clay and Friable Particles	Chert (Less Than 2.40 sp gr SSD)	Sum of Clay Lumps, Friable Particles, and Chert (Less Than 2.40 sp gr SSD)	Material finer than 75 µm	Coal and Lignite	Abrasion A	Soundness with magnesium sulphate (5 cycles) ^B
1S	Foundations, foundations and beams not exposed to the weather, internal floors from cover	10	1c	1	50	...
2S	Interior floors without coverings	5	1c	0.5	50	...
3S	Above-ground foundation walls, retaining walls, piers, beams and girders exposed to atmospheric agents	5	5	7	1c	0.5	50	18
4S	Floors, decks, driveways and kerbs, walkways, patios, garage floors, exposed floors and porches or front structures sea subject to frequent wetting	3	5	5	1c	0.5	50	18
5S	Architectural or decorative concrete a view	2	3	3	1c	0.5	50	18
<i>Moderate Weathering Regions</i>								
1M	Basements, foundations, pillars and beams not exposed to the weather, internal floors to be coated	10	1c	1	50	...
2M	Interior floors without coverings	5	1c	0.5	50	...
3M	Foundation walls above ground, retaining walls, pillars, beams and girders exposed to the atmospheric agents	5	8	10	1c	0.5	50	18
4M	Footpaths, decks, driveways and kerbs, walkways, patios, garage floors, exposed floors and porches or front structures sea subject to frequent wetting	5	5	7	1c	0.5	50	18
5M	Architectural or decorative concrete a view	3	3	5	1c	0.5	50	18
<i>Negligible Weathering Regions</i>								

1N	Sheets subject to traffic abrasion, decks, floors, pavements	5	1c	0.5	50	...
2N	All other concrete classes	10	1c	1	50	...

A- Crushed, air-cooled blast furnace slag is excluded from the abrasion requirements. The bulk density (unit weight) of crushed, air-cooled blast furnace slag shall not be less than 1120 kg/m³ [70 lb/ft³]. The classification of slag used in the bulk density (unit weight) test must be in accordance with the classification to be used in concrete. The abrasion loss of gravel, crushed stone or rubble shall be determined on the test size(s) closest to the classification(s) to be used in concrete. When more than one classification is to be used, the abrasion loss limit shall apply to each.

B- The limits allowed for test soundness should be 12 % if sodium sulphate is used.

C- This percentage under one of the following conditions: (1) may be increased to 1.5 if the material is essentially free of clay or shale; or (2) if it is known that the source of the fine aggregate to be used in the concrete contains less than the specified maximum amount which exceeds the 75 µm sieve (no. 200) the percentage limit (L) on the amount in the coarse aggregate may be increased to $L = 1 + [(P)/(100 - P)](T - A)$, where P = the percentage of sand in the concrete as a percentage of the total aggregate, T = the limit for the allowable amount in the fine aggregate and A = the actual amount in the fine aggregate. (This provides a weighted calculation designed to limit the maximum mass of material passing the 75 µm sieve (No. 200) in the concrete to that which would result if both the fine and coarse aggregate were supplied at the maximum percentage tabulated for each of these ingredients).

Aggregates for asphalts (Washington Department of Transportation 2004)

Particle characteristics

sieve opening (mm)	38.1	25.4	19.05	12.7	9.525	4.75	2.36	0.075
<i>loop (%)</i> (0.95 mm)				100	90-100	90 max	32-67	2-7
<i>loop (%)</i> (1.3 mm)			100	90-100	90 max		28-58	2-7
<i>loop (%)</i> (1.9 mm)		100	90-100	90 max			23-49	2-7
<i>loop (%)</i> (2.5 mm)	100	90-100	90 max				19-45	1-7

Physical characteristics

Los Angeles	35% - 50%
Plasticity index	From non-plastic to a maximum of 10
Soundness of fine and coarse	From 10% to 18%.
Absorption	4% to 6%

Portland cement (UNI-EN)

Commercially available cements mainly consist of mixtures of Portland cement with pozzolanic materials, hydraulically behaving pozzolanic materials and aggregate additions. In accordance with this standard, cements can be produced using the following main constituents:

- Portland cement clinker (K)
- Chalk
- Natural (P) and calcined natural (Q) pozzolans
- Silicic (V) and calcic (W) fly ash
- Granulated blast furnace slag (S)
- Microsilica or silica fume (D)
- Limestones (L or LL)
- Calcined shale (T)

Main types	Names of the 27 products (common cement types)		Composition (mass percentage ^{a)})												
			Main constituents										Secondary constituents		
			Clinker	Blast furnace slag	Silica smoke	Pozzolana		Ash steering wheel		Calcined shale	Limestone				
						Natural	Natural calcined	Silicea	Limestone		L	LL			
K	S	Dbj	P	Q	V	W	T	L	LL						
CEM I	Portland cement	CEM I	95-100	-	-	-	-	-	-	-	-	-	-	-	0-5
EMC II	Portland cement with slag	CEM II/A-S	80-94	6-20	-	-	-	-	-	-	-	-	-	-	0-5
		CEM II/B-S	65-79	21-35	-	-	-	-	-	-	-	-	-	-	0-5
	Portland cement to silica fumes	CEM II/A-D	90-94	-	6-10	-	-	-	-	-	-	-	-	-	0-5
		CEM II/A-P	80-94	-	-	6-20	-	-	-	-	-	-	-	-	0-5

Portland cement with pozzolan	CEM II/B-P	65-79	-	-	21-35	-	-	-	-	-	-	-	0-5
	CEM II/A-Q	80-94	-	-	-	6-20	-	-	-	-	-	-	0-5
	CEM II/B-Q	65-79	-	-	-	21-35	-	-	-	-	-	-	0-5
Fly ash Portland cement	CEM II/A-V	80-94	-	-	-	-	6-20	-	-	-	-	-	0-5
	CEM II/B-V	65-79	-	-	-	-	21-35	-	-	-	-	-	0-5
	CEM II/A-W	80-94	-	-	-	-	-	6-20	-	-	-	-	0-5
	CEM II/B-W	65-79	-	-	-	-	-	21-35	-	-	-	-	0-5

	Portland cement calcined shale	CEM II/A-T	80-94	-	-	-	-	-	-	6-20			0-5
		CEM II/B-T	65-79							21-35			0-5
	Limestone Portland cement	CEM II/A-L	80-94	-	-	-	-	-	-	--	6-20	-	0-5
		CEM II/B-L	65-79	-	-	-	-	-	-	-	21-35	-	0-5
		CEM II/A-LL	80-94	-	-	-	-	-	-	-	-	6-20	0-5
		CEM II/B-LL	80-94	-	-	-	-	-	-	-	-	21-35	0-5
Portland cement composite	CEM II/A-M	80-88	12-20									0-5	
	CEM II/B-M	68-79	21-35										
EMC III	Blast furnace cement	CEM III/A	35-64	36-50	-	-	-	-	-	-	-	-	0-5
		CEM III/B	20-34	66-80	-	-	-	-	-	-	-	-	0-5
		CEM III/C	5-19	81-95	-	-	-	-	-	-	-	-	0-5
CEM IV	Pozzolanic cement ^{c)}	CEM IV/A	65-89	-	11-65				-	-	-	0-5	
		CEM IV/B	45-64	-	36-55				-	-	-	0-5	
CEM V	Composite cement ^{c)}	CEM V/A	40-64	18-30	18-30		-	-	-	-	-	0-5	
		CEM V/B	20-38	31-49	31-49		-	-	-	-	-	0-5	
<p>a. The values in the table refer to the sum of the main and secondary constituents</p> <p>b. The proportion of silica fume is limited to 105</p> <p>c. In CEM II/A-M and CEM II/B-M composite Portland cements, CEM IV/A and CEM IV/B pozzolanic cements and CEM composite cements V/A and CEM V/B main constituents other than clinker must be declared by cement designation (e.g. see item 8)</p>													

Soil correction (ASTM)

Using carbonate rocks, a process of soil de-acidification can be implemented.

The first prerequisite for using the material for this purpose is therefore that the lithology of the deposit consists of limestone and/or dolomite.

Particle size characteristics

The grain distribution with 95% less than 0.85 mm, 60% less than 0.25 mm and 50% less than 0.15 mm.

Some countries require 75/100% of the material to be less than 2/2.38 mm and 25% to be less than 0.25 mm

Bibliography

3GSM GmbH (<https://3gsm.at/de/produkte/bmx-fragmenter/>)

Bischoff, Christine Anna; Ghail, Richard C.; Mason, Philippa J.; Ferretti, Alessandro; Davis, John A. (2020): Revealing millimetre-scale ground movements in London using SqueeSAR™. In *Quarterly Journal of Engineering Geology and Hydrogeology* 53 (1), pp. 3–11. DOI: 10.1144/qjgeh2018-075.

Brardinoni F, Slaymaker O, Hassan MA. 2003. Landslide inventory in a rugged forested watershed: a comparison between air-photo and field survey data. *Geomorphology* 54: 179–196. DOI: 10.1016/S0169-555X (02)00355-0

Brardinoni F. e Cavalli M., 2012. Classification Scheme for Colluvial Sediment Sources. Technical note progetto SedAlp, pp. 2.

Castiglioni G.B., 1996. Geomorfologia, UTET.

Cousot, Ph., Meunier, M., 1996. Recognition, classification, and mechanical description of debris flows. *Earth-Science Reviews* 40, 209-227.

Dörfler, Markus (2020): InSAR Competence Center. GEORESEARCH Forschungsgesellschaft mbH. Available online at <http://www.georesearch.ac.at/en/areas/insar-competence-center/insar-competence-center/>, checked on 11/09/2022.

Dörfler, Markus (2022): Analysis of aquifer-induced soil movements of heterogeneous subsoil in urban areas based on groundwater, borehole and InSAR data, a case study of Salzburg. Master Thesis. Paris-Lodron-University of Salzburg

FASTVEL (2022): FASTVEL for displacement velocity map generation, Available online: <https://terradue.github.io/doc-tep-geohazards-v2/tutorials/fastvel.html>

Ferretti, Alessandro (2007): InSAR principles. Guidelines for SAR interferometry : processing and interpretation. Noordwijk: ESA publications.

Ferretti, Alessandro; Fumagalli, Alfio; Novali, Fabrizio; Prati, Claudio; Rocca, Fabio; Rucci, Alessio (2011): A New Algorithm for Processing Interferometric Data-Stacks: SqueeSAR. In *IEEE Trans. Geosci. Remote Sensing* 49 (9), pp. 3460–3470. DOI: 10.1109/TGRS.2011.2124465.

- Ferretti, Alessandro (2014): Satellite InSAR Data. Reservoir monitoring from space. Houten: EAGE Publications bv (Educational tour series, [ISSN 1879-5064], 9).
- GBA (2002): Allgemeine Informationen zu Massenbewegungen. Geologische Bundesanstalt Wien. Online available:
https://www.geologie.ac.at/fileadmin/user_upload/dokumente/pdf/service/webapplikation/allgemeine_info_mass_end_h.pdf
- Intrieri, Emanuele; Raspini, Federico; Fumagalli, Alfio; Lu, Ping; Del Conte, Sara; Farina, Paolo et al. (2018): The Maoxian landslide as seen from space: detecting precursors of failure with Sentinel-1 data. In *Landslides* 15 (1), pp. 123–133. DOI: 10.1007/s10346-017-0915-7.
- Kogel, J. E., Trivedi, N. C., Barker, J. M., & Krukowski, S. T. (Eds.). (2006). Industrial minerals & rocks: commodities, markets, and uses. SME.
- Koudogbo, Fifamè et al. (2018): Radar interferometry as an innovative solution for monitoring the construction of the Grand Paris Express metro network – First results.
- Krauter, E. (1990): Phänomenologie natürlicher Böschungen (Hänge) und ihre Massenbewegungen. In: Grundbau-Taschenbuch, 4. Aufl., 1. Berlin (Ernst&Sohn). S. 565-614;
- Liao, Mingsheng; Balz, Timo; Rocca, Fabio; Li, Deren (2020): Paradigm Changes in Surface-Motion Estimation From SAR: Lessons From 16 Years of Sino-European Cooperation in the Dragon Program. In *IEEE Geosci. Remote Sens. Mag.* 8 (1), pp. 8–21. DOI: 10.1109/MGRS.2019.2956176.
- Novellino, Alessandro; Cigna, Francesca; Brahmi, Mouna; Sowter, Andrew; Bateson, Luke; Marsh, Stuart (2017): Assessing the Feasibility of a National InSAR Ground Deformation Map of Great Britain with Sentinel-1. In *Geosciences* 7 (2), p. 19. DOI: 10.3390/geosciences7020019.
- Osmanoğlu, Batuhan; Dixon, Timothy H.; Wdowinski, Shimon; Cabral-Cano, Enrique; Jiang, Yan (2011): Mexico City subsidence observed with persistent scatterer InSAR. In *International Journal of Applied Earth Observation and Geoinformation* 13 (1), pp. 1–12. DOI: 10.1016/j.jag.2010.05.009.
- RFI, TECHNICAL TENDER GENERAL FOR CONTRACTING CIVIL WORKS - PART II - SECTION 17 STONEWARE FOR RAILWAY FACILITIES - 31/12/2020 (<https://www.rfi.it/content/dam/rfi/fornitori-e-tenders/qualification-economic-operators/list-suppliers-pietrisco/Capitolato%20->

[%20Part%20II%20-%20Sezione%2017%20-%20Pietrisco%20per%20massicciata%20ferroviaria.pdf](#)

ShapeMetriX (Fragmenter Tool) from the company 3GSM GmbH (<https://3gsm.at/de/produkte/bmx-fragmenter/>).

Software PFC2D (<https://www.itascacg.com/software/PFC>)

TRE ALTAMIRA (2018): Handbook. TRE ALTAMIRA InSAR Products. HDB 2.2.

Tscharf, A.: UAV-gestützte Vermessung im Bergbau – Zur Frage der Genauigkeit unter Verwendung von Structure from Motion, Diss., Leoben, Montanuniv., Lehrst. F. Bergbaukunde, Bergtechnik und Bergwirtschaft, 2020

UNI EN 197-1:2011 COMPOSITION, SPECIFICATIONS AND CONFORMITY CRITERIA FOR COMMON CEMENT
<https://www.azichem.com/news/uni-en-197-1-2011-composizione-specificazioni-e-criteri-di-conformance%C3%A0-for-common-cements/249/>

US Geological Survey, 2004. Landslide Types and Processes, Fact Sheet 2004-3072.

Varnes D.J., 1978. Slide movement types and processes. Landslides, Analysis and Control, Transportation Research Board, Special Report No. 176, National Academy of Sciences, 11-33.